First principles-based moiré model for incommensurate graphene on BN

SAND2016-4819PE

Catalin Spataru

Konrad Thurmer

Materials Physics Dept.

Sandia National Laboratories

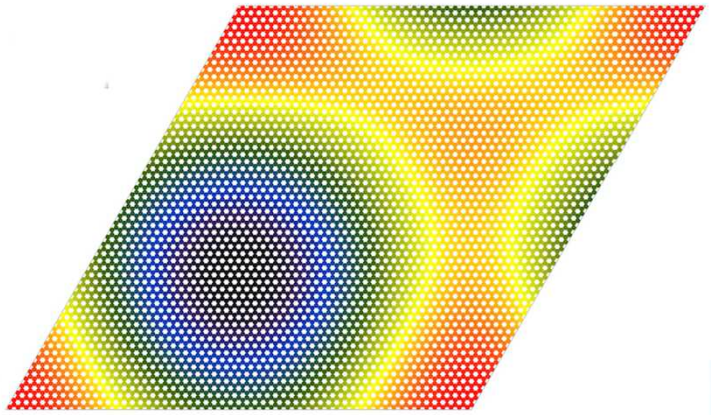

Introduction

- Various properties of **graphene** depend strongly on the underlying **substrate**:
  - electronic, optical, transport, etc..

- **BN** is substrate of choice for graphene devices:
  -large smooth areas due to strong intra- and weak inter-layer bonding.
  -less charged impurities, small charge puddle fluct.

- **C/BN** → band gap as large as 30 meV[1]:
  -commensurate domains[1].
  -many-electron effects[2].

- **Atomic structure not well understood**:
  - max. corugation: 0.2 Å (theory[2,3]) vs. 0.4 to 3 Å (exp.[4,5]).

AFM image[4]:

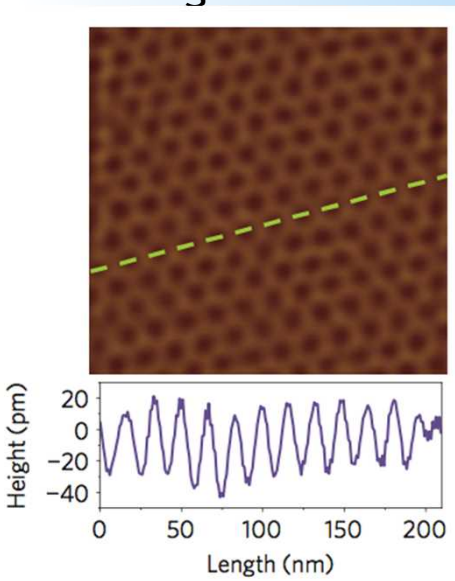

STM image[5]:

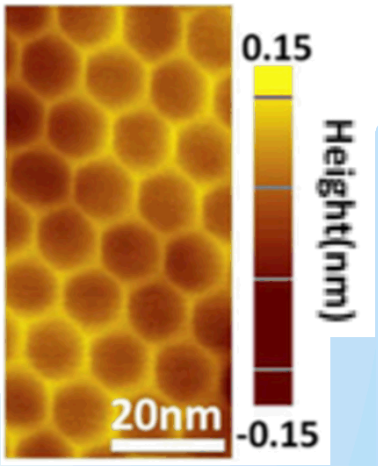

1) Woods et al. Nature Phys. **10** 451 (2014).
2) Bokdam et al. PRB **89** 201404 (2014).
3) Jung et al. Nat. Comm. **6** 6308 (2015).
4) Yang et al. Nano Lett. **12** 792 (2013).
5) Lu et al. PRL **113** 156804 (2014) .

Motivation

- **Desired: atomic structures** with state-of-the-art **DFT accuracy**.

-weak interaction + small **lattice mismatch ~1.8%** → large moiré structures cannot be treated with *ab initio* DFT.

✓ DFT-based **moiré** model for **incommensurate graphene on BN**:

-large moiré periodicity.

-various relative azimuthal orientation.

Ab initio approach

- Density Theory Functional (**DFT**) within local density approx. (LDA[1]).
  -impact of van der Waals corrections checked via Grimme's method[2].

- Projector augmented wave (PAW) pseudopotentials[3] as implemented in **VASP**[4].

Supercell with **1 graphene** layer on top of **3 hBN** layers:

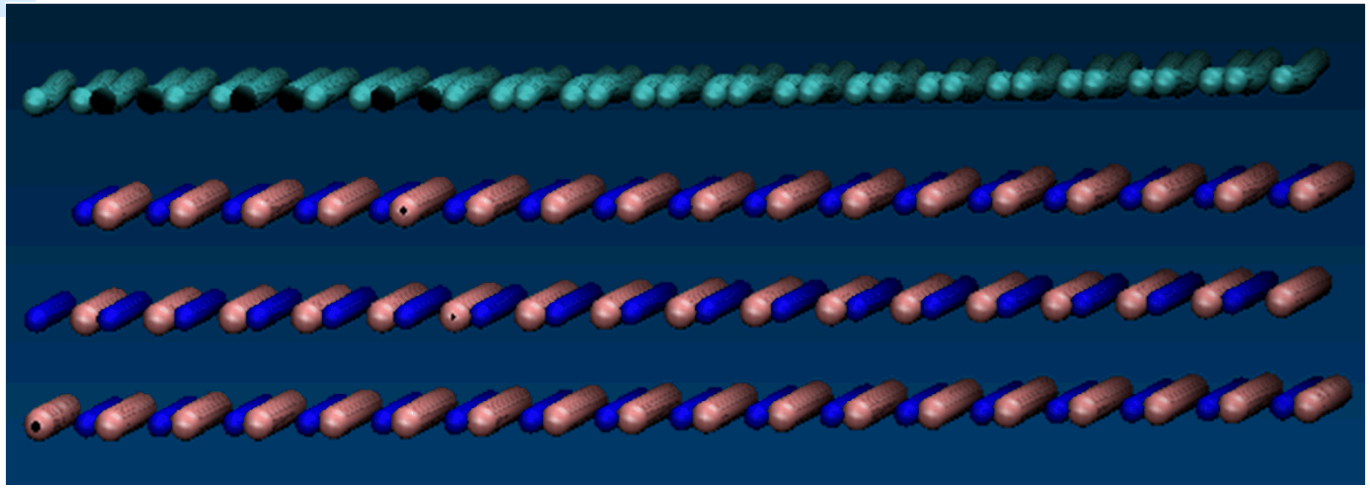

allowed to relax

unrelaxed

✓ Relaxed **forces < 1 meV/Å.**

1) Kohn and Sham, *Phys. Rev.* (1965).
2) Grimme, *J. Comp. Chem.* **27**, 1787 (2006).
3) Blöchl, *Phys. Rev. B* **50**, 17953 (1994). Kresse, and Joubert, *Phys. Rev. B* **59**, 1758 (1999).
4) Kresse and Furthmuller, *Phys. Rev. B* **54**, 11169 (1996).

Moiré model

- Substrate (BN) is represented by a sum of **sinusoids**
  → **potential minima** z_0.

- Assume **harmonic** graphene-substrate interaction.

- Intra-graphene forces F_{flex} derived from calculated **flexural rigidity**.

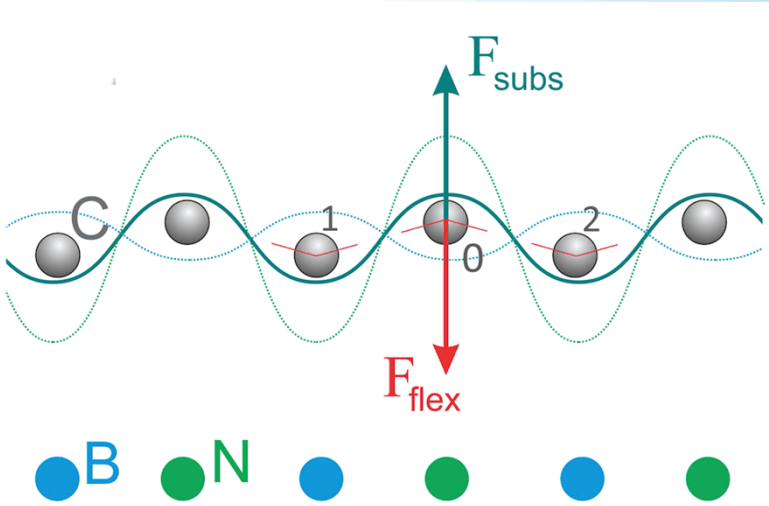

- F_{flex} is **balanced** by the force from substrate interaction.

Harmonic C-BN interaction: $\delta E = 1/2\, k_{\text{inter}} \delta z^2$

LDA **total energy** of **flat** 15 C/14 BN (var. separations) → k_{inter}

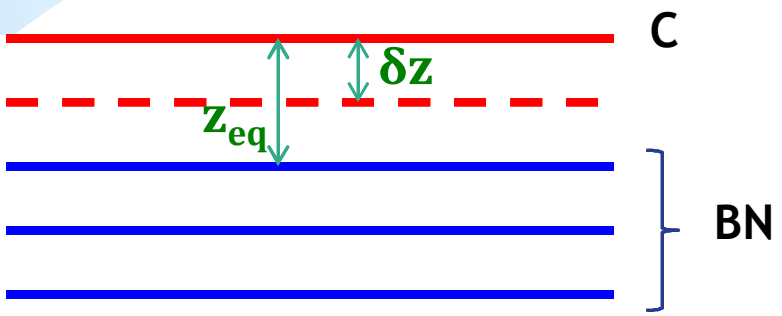

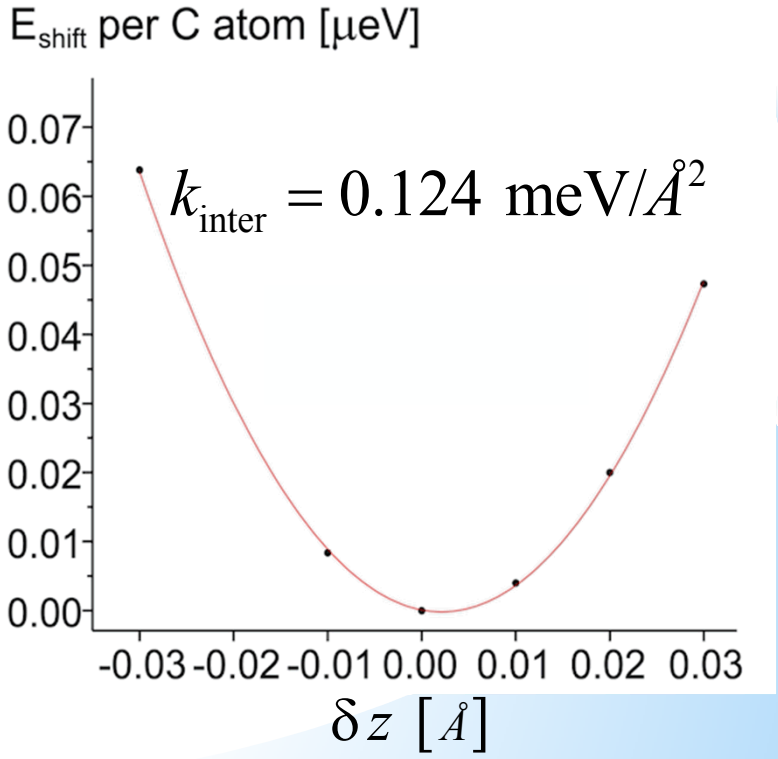

Flexural force due to change in bond angle:

$$F_{flex} = -k_{flex}[z - f(z_{neighborsI,II})]$$

LDA **forces** for a reasonable initial guess of corrugated graphene → k_{flex}

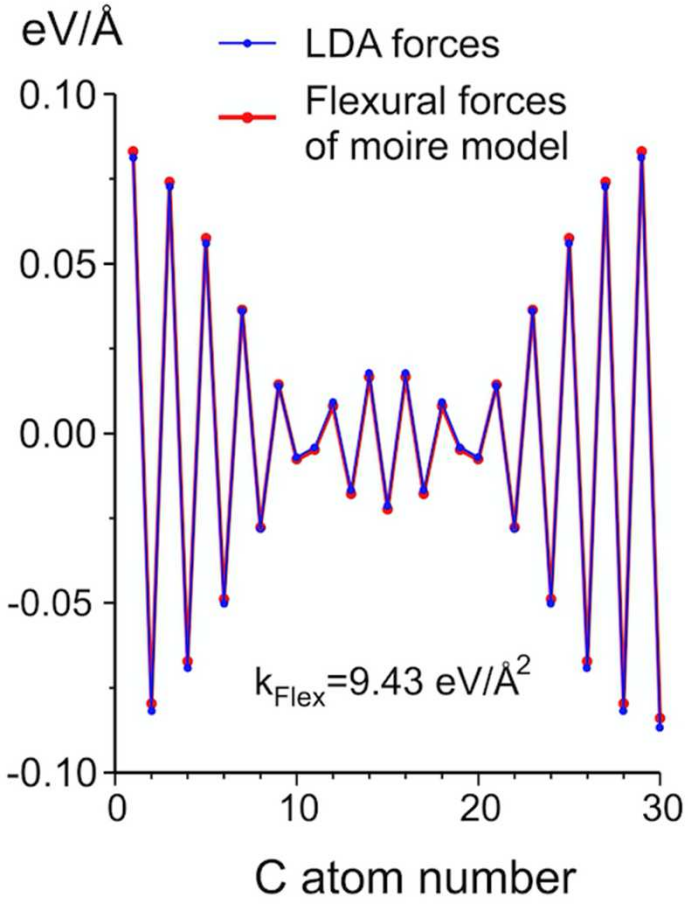

Force from substrate interaction: $F_{subs} = -k_{\text{inter}}(z - z_0)$

$$z_0 = A_B \sum_{G}^{|G|=2\pi/a_{BN}} \sin(G_x x + G_y y + \varphi_B) + A_N \sum_{G}^{|G|=2\pi/a_{BN}} \sin(G_x x + G_y y + \varphi_N)$$

LDA **forces** of **flat** 15 C/14 BN → A_B, A_N

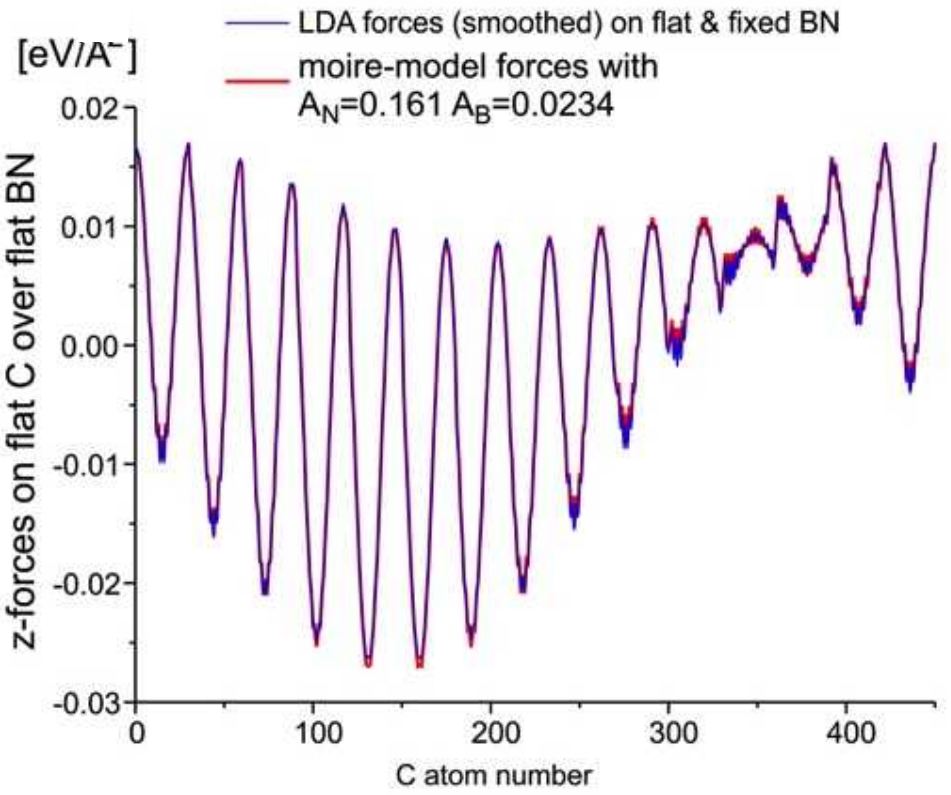

- **Benchmark** moiré model against LDA for several **rotations** of C/BN.
  -strained BN lattice to accommodate manageable supercell size.

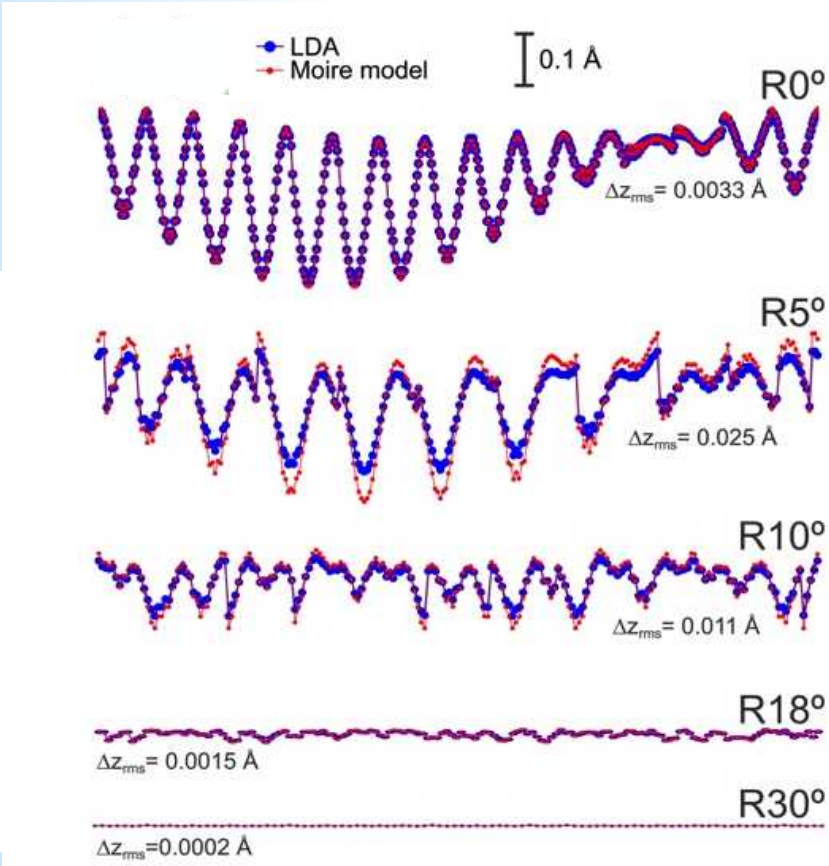

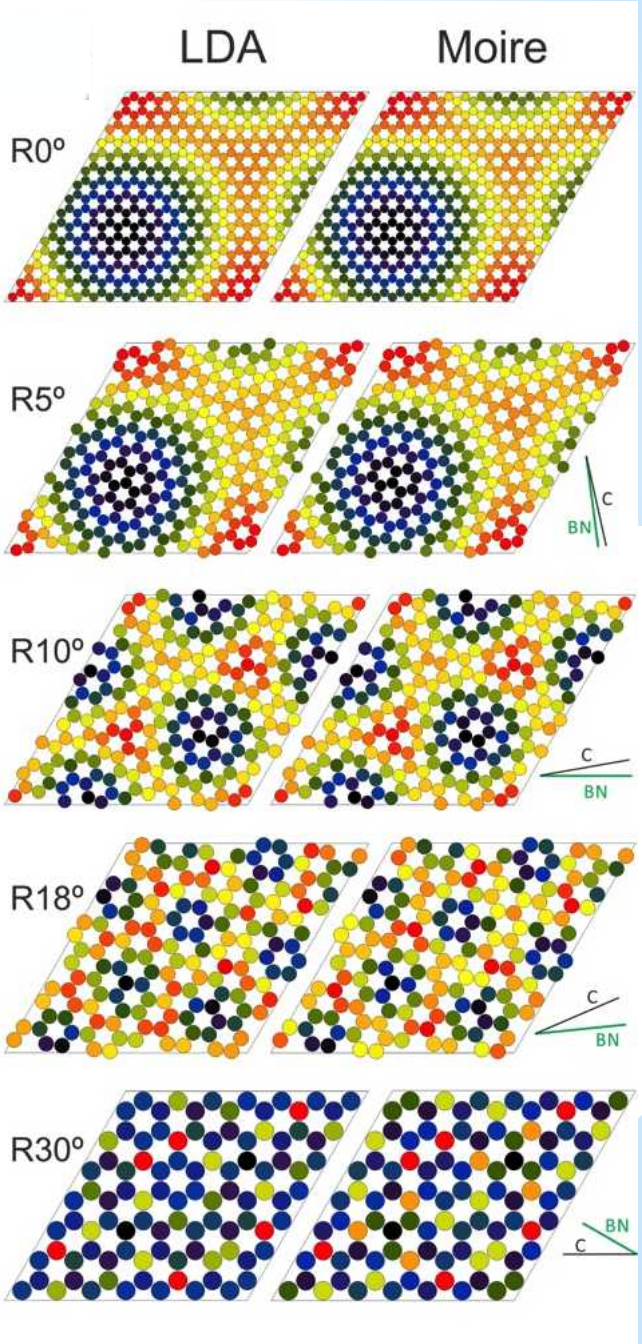

- Non-adjustable 4-parameter model reproduces LDA C-positions (**relative** to BN) of hundreds of atoms with ~ 0.01 Å accuracy.

- Apply moiré model to **unstrained** C/BN systems that are not doable via DFT.
- Predict **structure** and **energy**:

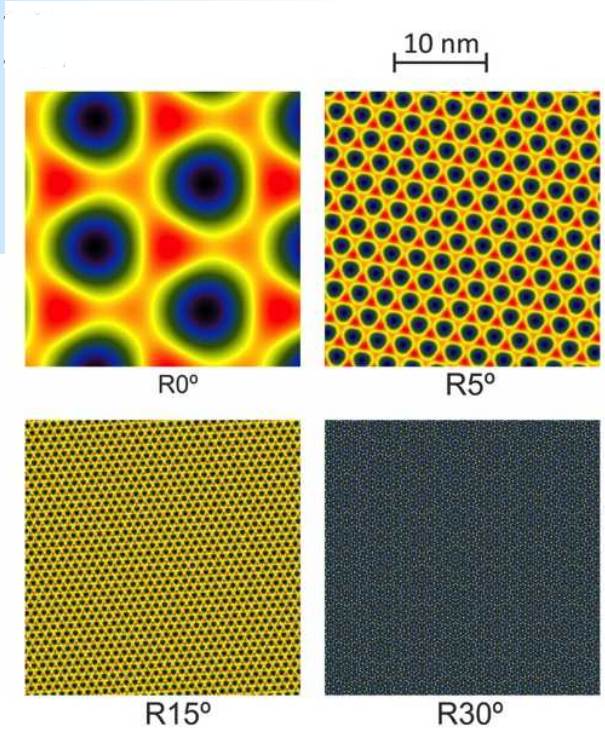

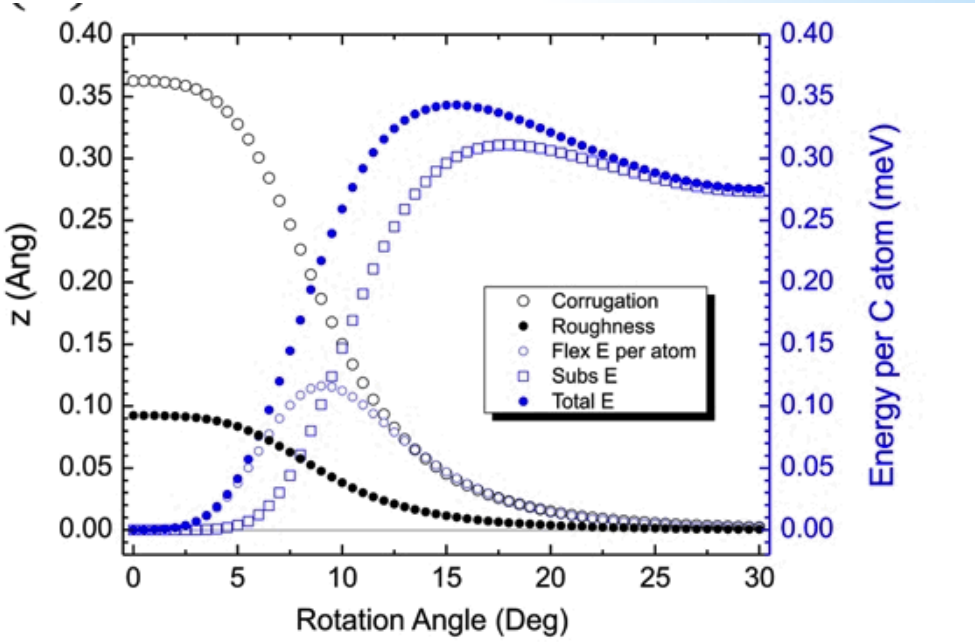

- **small-angles** are most favorable.
- **energy cost** for rotation is similar to the one measured for **C/Ir**[1].
- **in-plane relaxation** not included in energy; this might affect local minimum at 30°.

1) Rogge et al. Nat.Comm. **6** 6880 (2015).

- Unrotated **14 nm** moiré (C/BN 57/56):

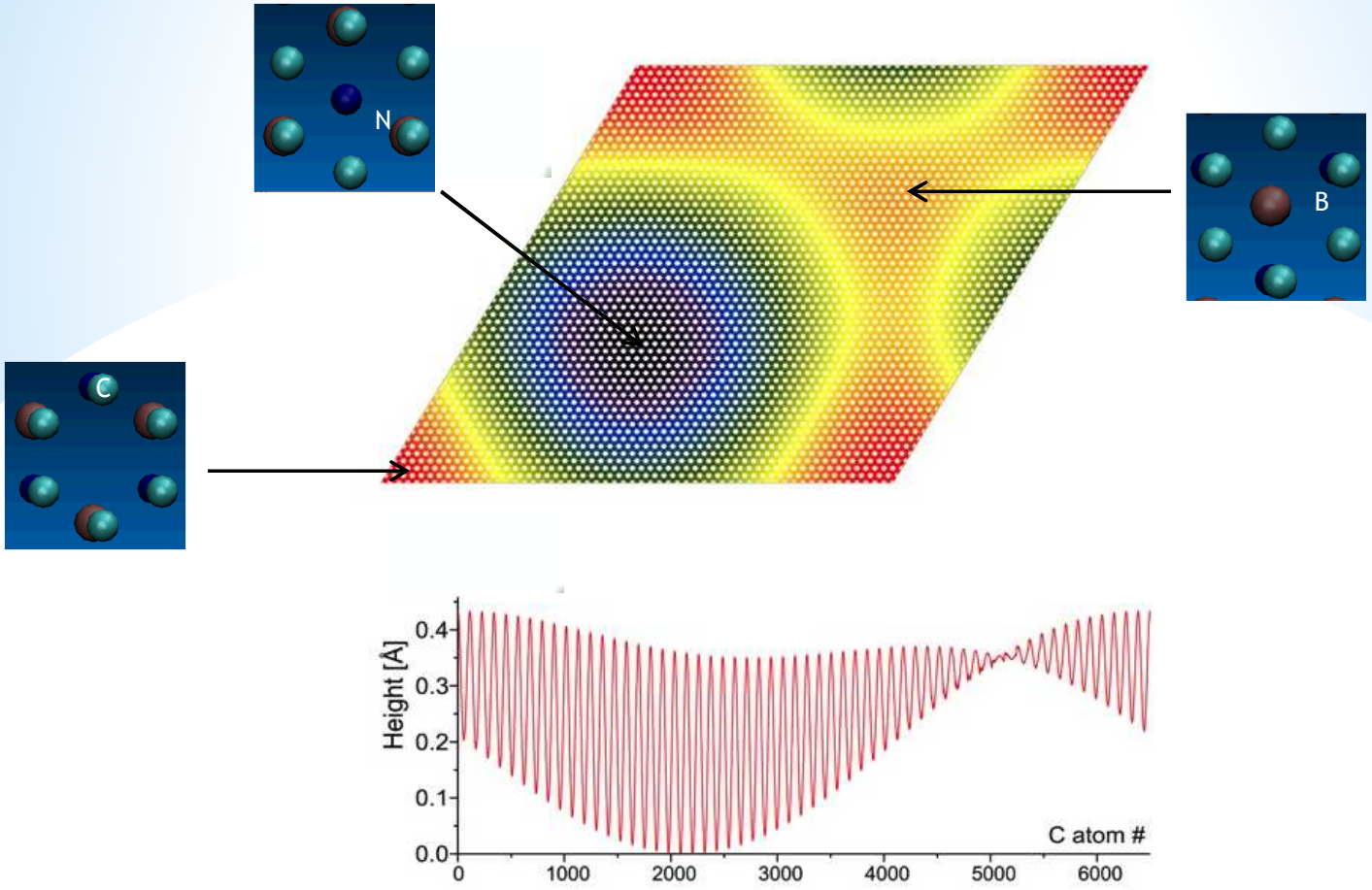

- Absolute **corrugation**: **0.42 Å** (takes into account relaxation of BN).
- **Frenkel-Kontorova** model for **in-plane** relaxation: **no** commensurate domains/sharp boundaries.

Frenkel-Kontorova model applied to 37 nm moiré (C/BN 148/147):

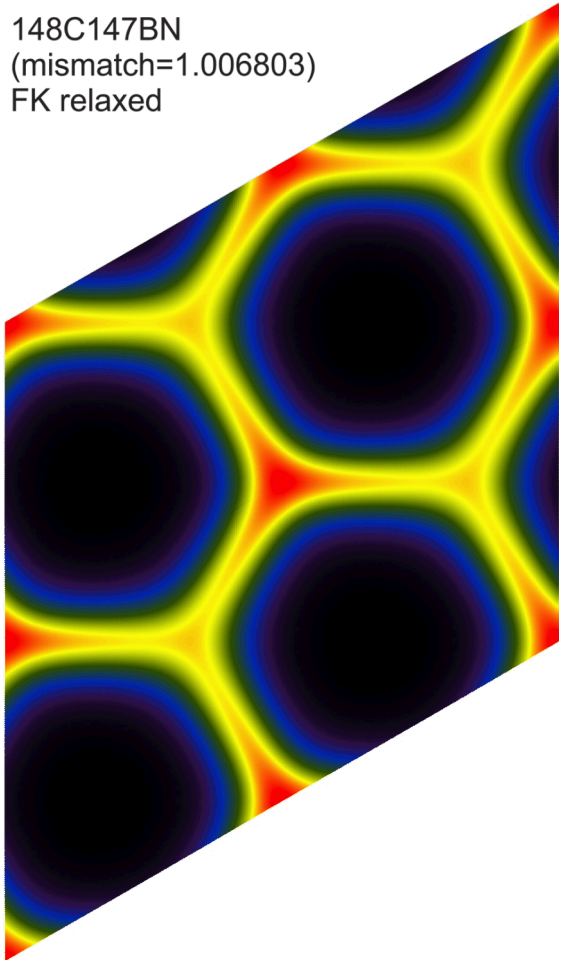

AFM image[1)]

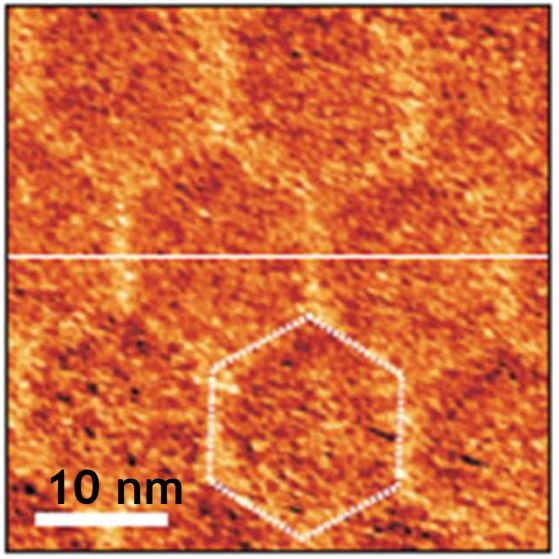

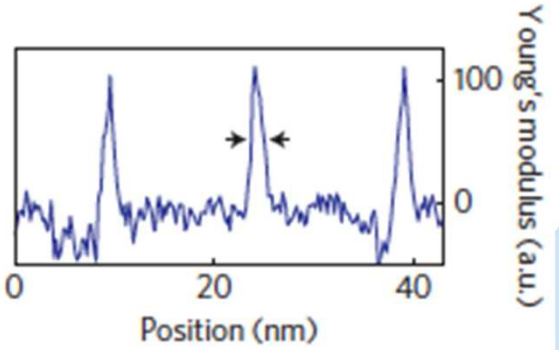

- **Sharp boundaries** obtained only for **unrealistically large** moiré.

1) Woods et al. Nature Phys. **10** 451 (2014)

Summary

- Non-adjustable 4-parameter moiré model predicts **C/BN** atomic structures close to DFT-accuracy.
  - can be applied to **other heterostructure** systems.
- Max. corrugation for C/BN: 0.4 Å.
- Small rotation angles are most favorable energetically.

Future work:

- Use moiré model to inform first principle calculations of small, **commensurate** systems → parameterize a tight-binding Hamiltonian.
  -predict electronic structure, optical properties, etc..

Acknowledgements

Thomas Beechem (Sandia)

LDRD
Laboratory Directed Research & Development

Sandia National Laboratories is a multi-program laboratory managed and operated by Sandia Corporation, a wholly owned subsidiary of Lockheed Martin Corporation, for the U.S. Department of Energy's National Nuclear Security Administration under contract DE-AC04-94AL85000.

First Principles-Based Modeling of Metal Contacts in Thermoelectric Materials and Devices

Catalin Spataru, François Léonard, Doug Medlin, Yuping He

Sandia National Labs

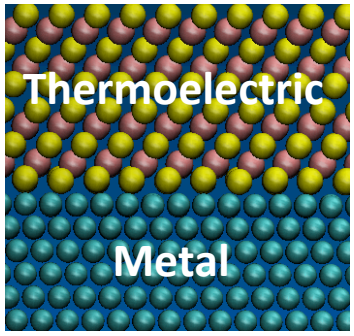

Introduction

Metal-TE contacts.

- important for **thin-film** thermoelectric devices for **high heat-flux** applications (*e.g.* chip cooling).
  - reduced **contact resistivity** (Joule heating) is critical to device performance.

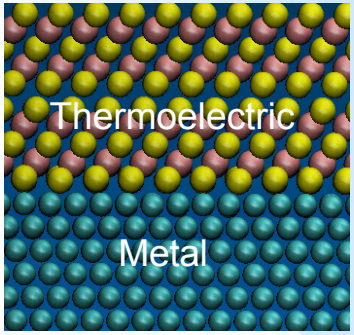

✓ **First principles-based approach to study the properties of electrical contacts to TE materials.**

→help bridge the gap between materials and devices.

→work with device performers to achieve better metal contacts.

* Motivation

Metallized epitaxial Bi_2Te_3/Sb_2Te_3 device structures provided to Sandia. (Courtesy of **Philip Barletta, RTI**)

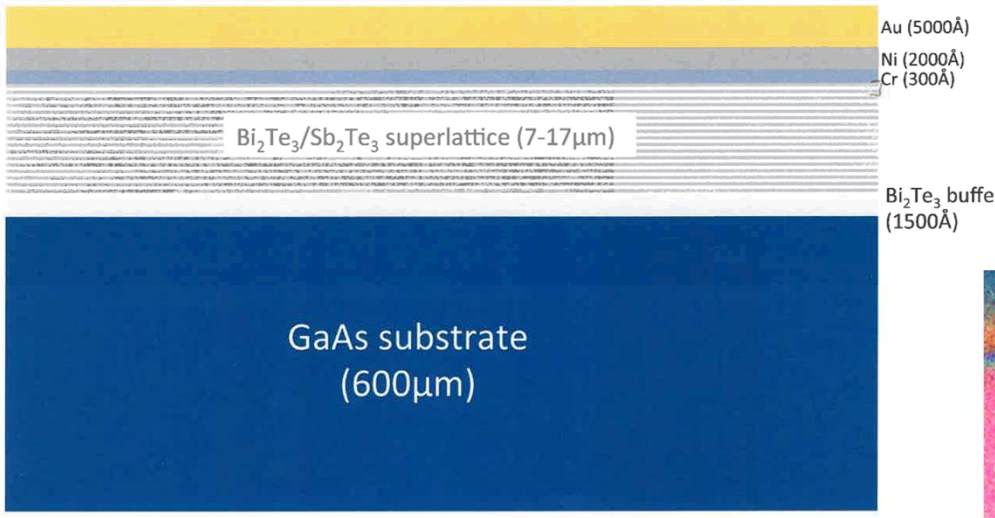

FIB/SEM cross-section:

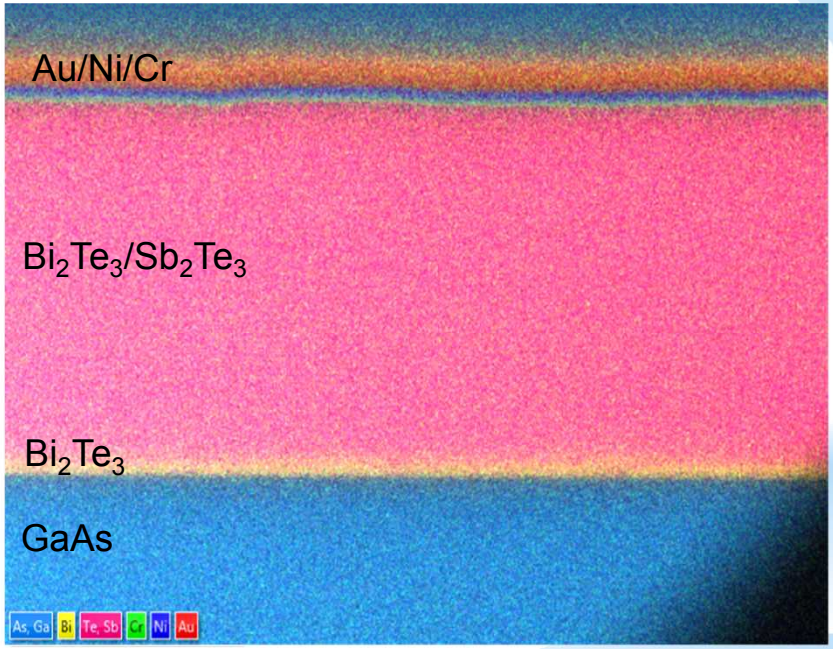

5 micron

Measured ρ_c ~ 10^{-7} to $10^{-6}\Omega cm^2$

Goal: $\rho_c < 10^{-8}\Omega cm^2$

What is the fundamental limit of contact resistivity ?

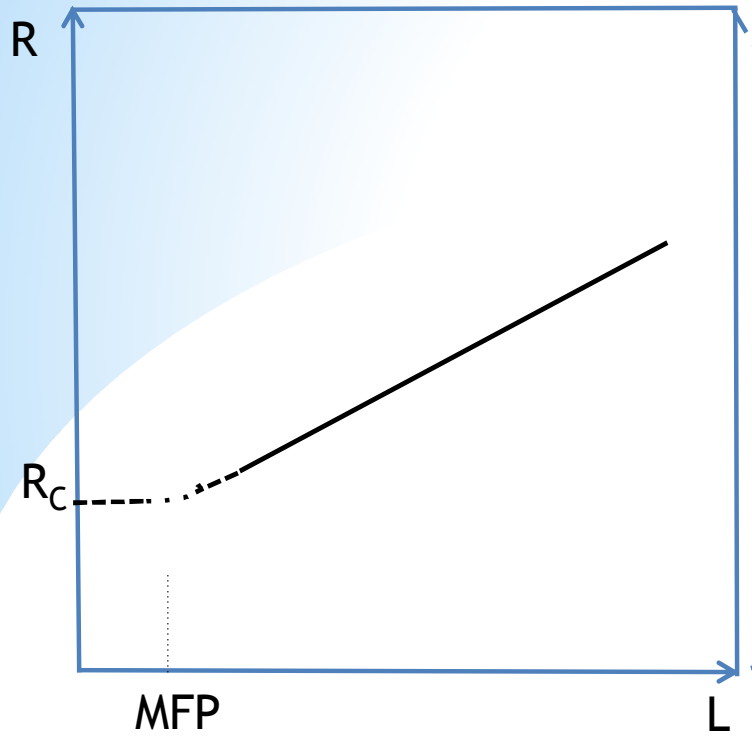

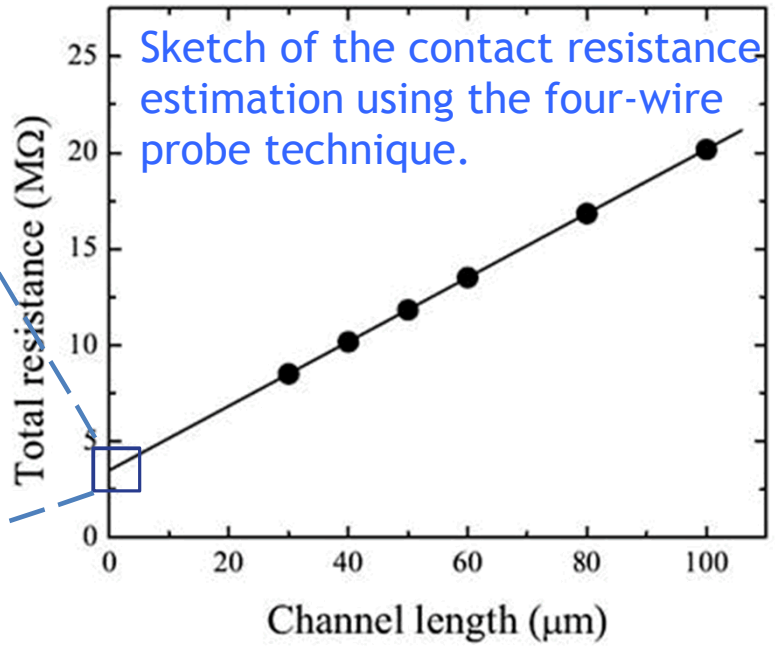

- TE resistivity in **balistic** regime → $\rho_C^{\min}$.

$$\rho_C^{\min} = R_0 / DOM$$

- R_0=12.9 kΩ
- DOM=# of modes/unit area

Density of modes for TE

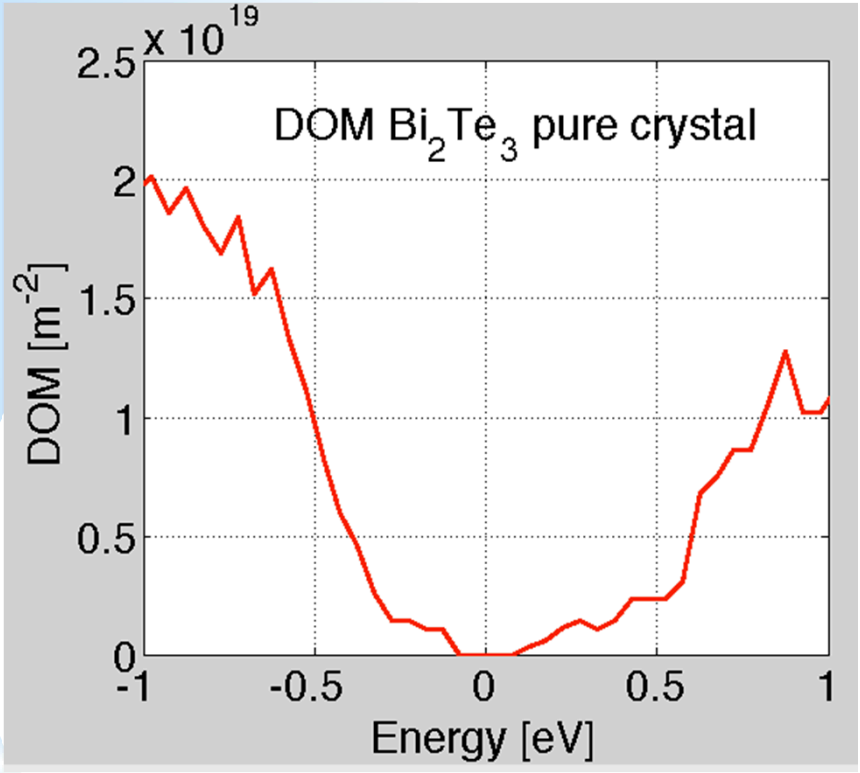

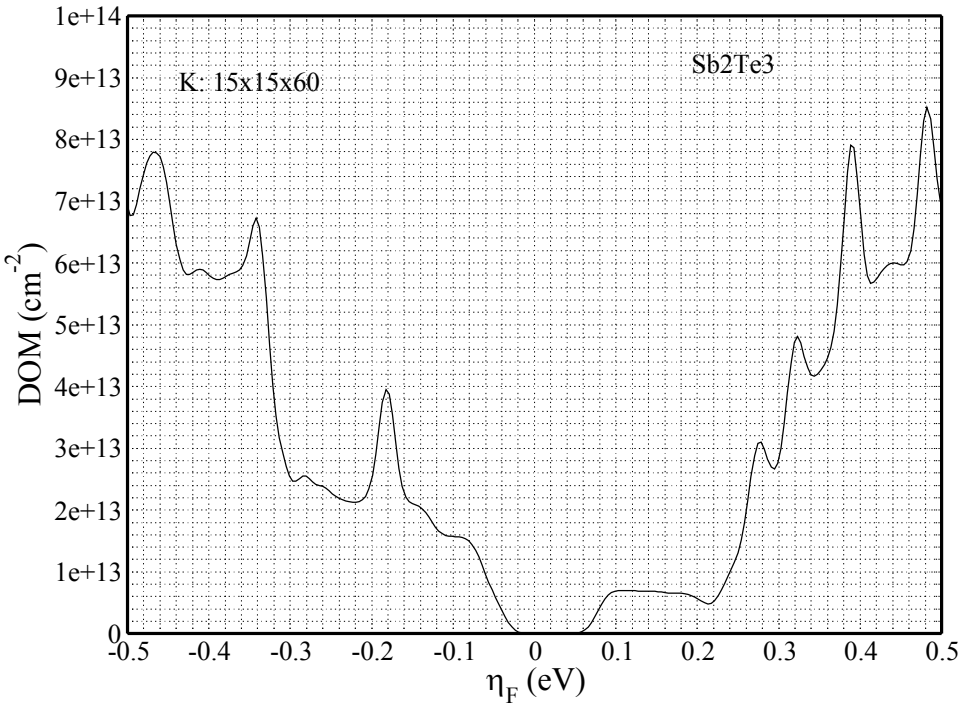

Bi_2Te_3 : $\rho_c^{\min} \sim 10^{-10}\,\Omega \times \mathrm{cm}^2$ at p~10^{19}holes/cm^3.

Jeong, Kim, Luisier, Datta and Lundstrom, JAP **107**, 023707 (2010).

Reflectionless metal contact:

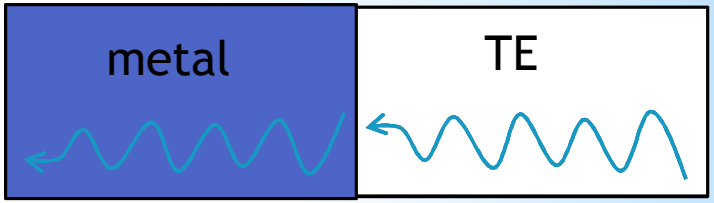

- metal DOM >> TE DOM.
- for every mode ($k_{||}$, k_{perp},E) in the TE, there is a corresponding mode in the metal.
  → no mode scattering at contact.

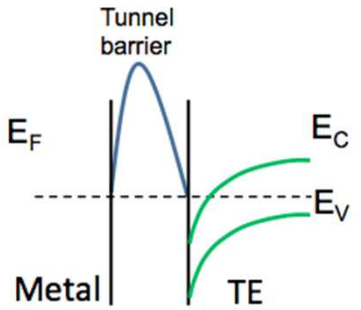

Real materials:

- metal and TE have different chemical potential:
  → charge transfer, **eletrostatic barrier**.

- materials have atomic structure:
  → **bandstructure mismatch effects**.

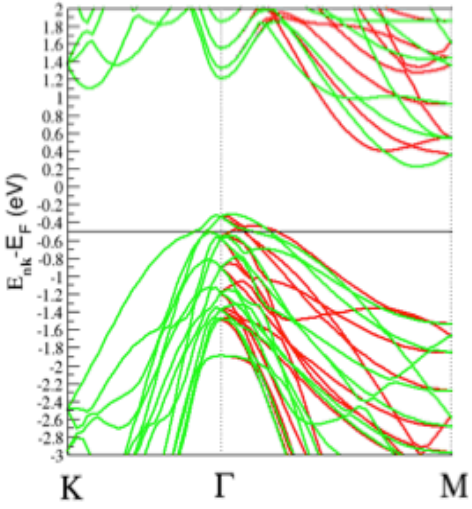

Twin boundary in Si: Electronic bandstructure of a Si single crystal for $k_{||}$ along two directions. Green lines → unrotated Si crystal. Red lines → crystal rotated 180° about the z-axis.

- other effects: **disorder**, atomic roughness, inter-diffusion, mixed interfacial phase, oxidation, e

Ab initio calculations

✓ Electronic properties of bcc **Cr,** fcc **Ti**, **Bi_2Te_3**, **Sb_2Te_3**.
- bulk and slab (several surfaces), superlattice.

Cr bulk

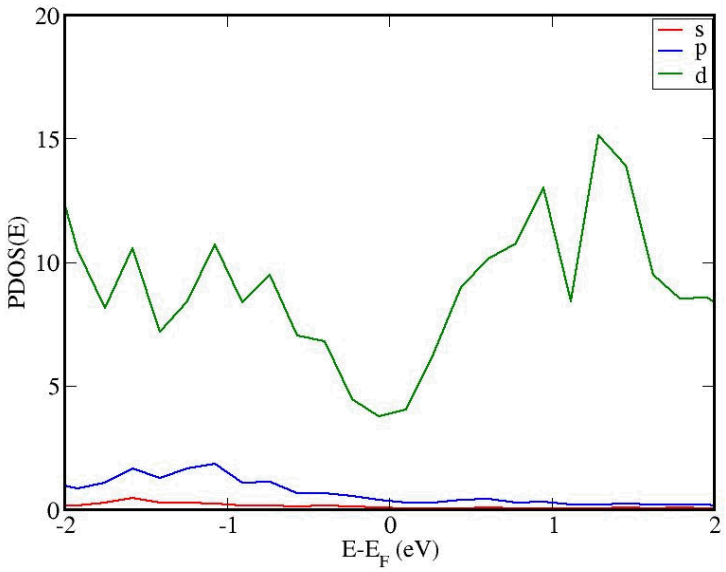

Bi_2Te_3 slab (3QP)

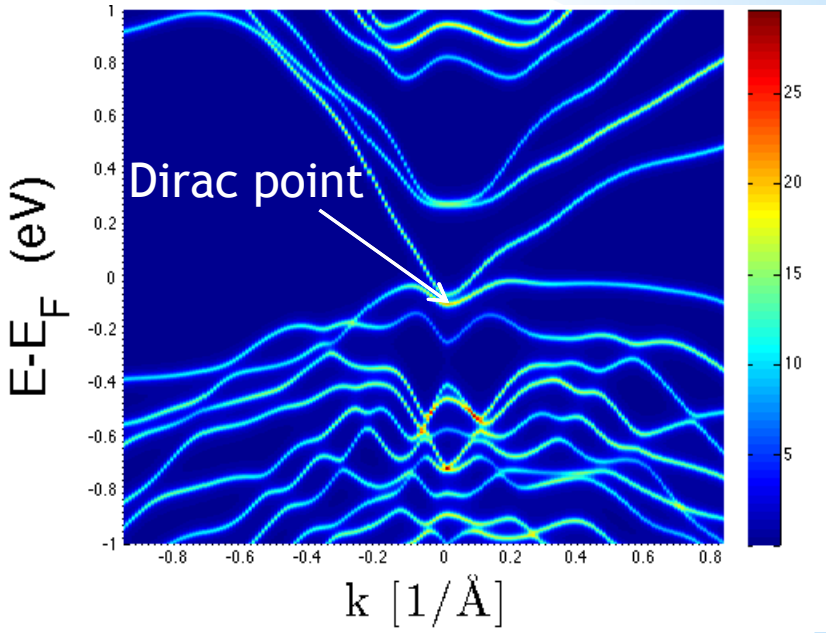

- **High density** of d-electron states.
  - expect that band-structure mismatch effects not important.

- Top. Ins. → **metallic surfaces** states.

Use **VASP** code: Kresse and Furthmuller, *Phys. Rev. B* **54**, 11169 (1996).

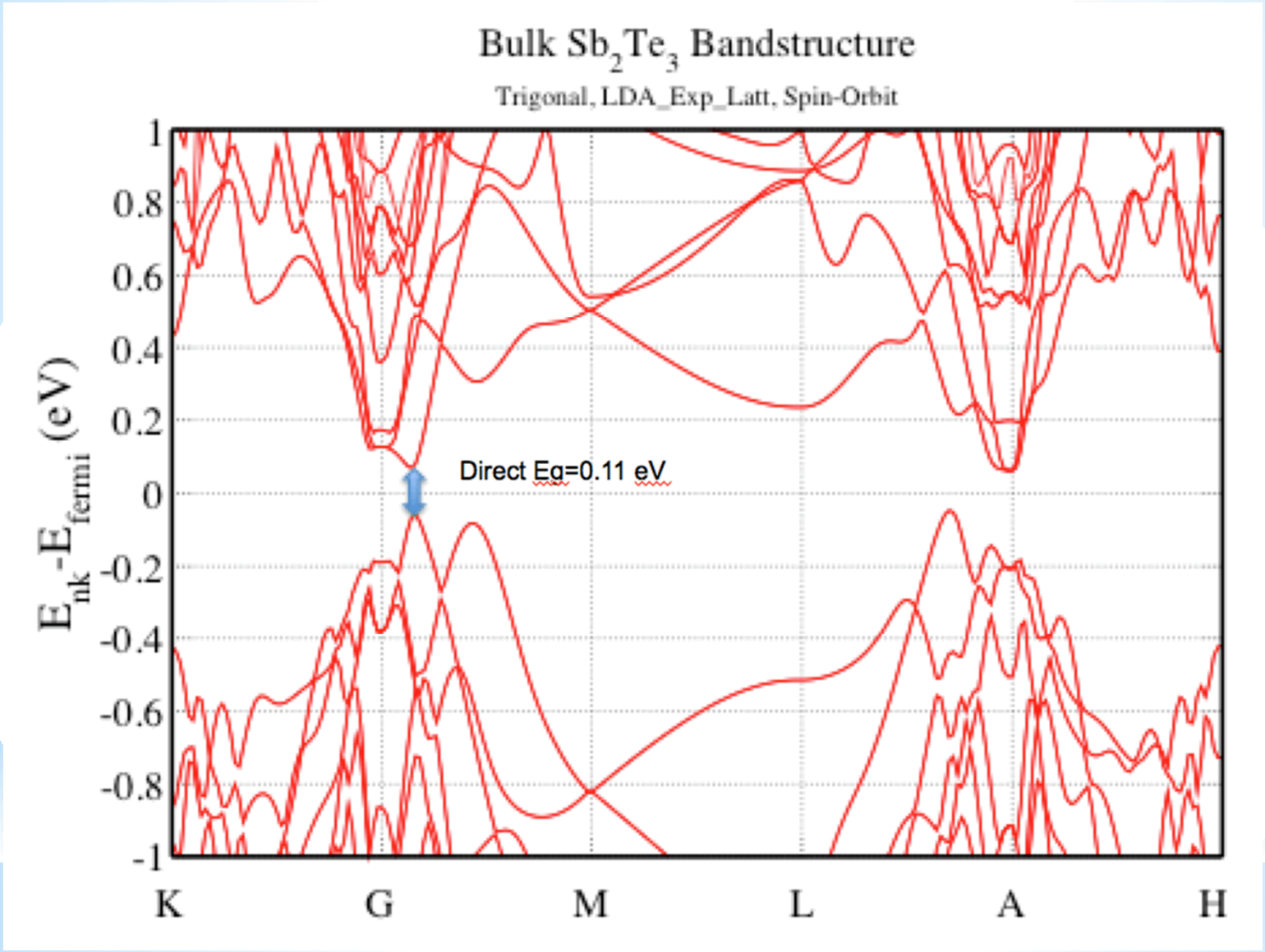
Bulk Sb2Te3 Bandstructure
Trigonal, LDA_Exp_Latt, Spin-Orbit
Direct Eg=0.11 eV
E_nk-E_fermi (eV)
1
0.8
0.6
0.4
0.2
0
-0.2
-0.4
-0.6
-0.8
-1
K
G
M
L
A
H

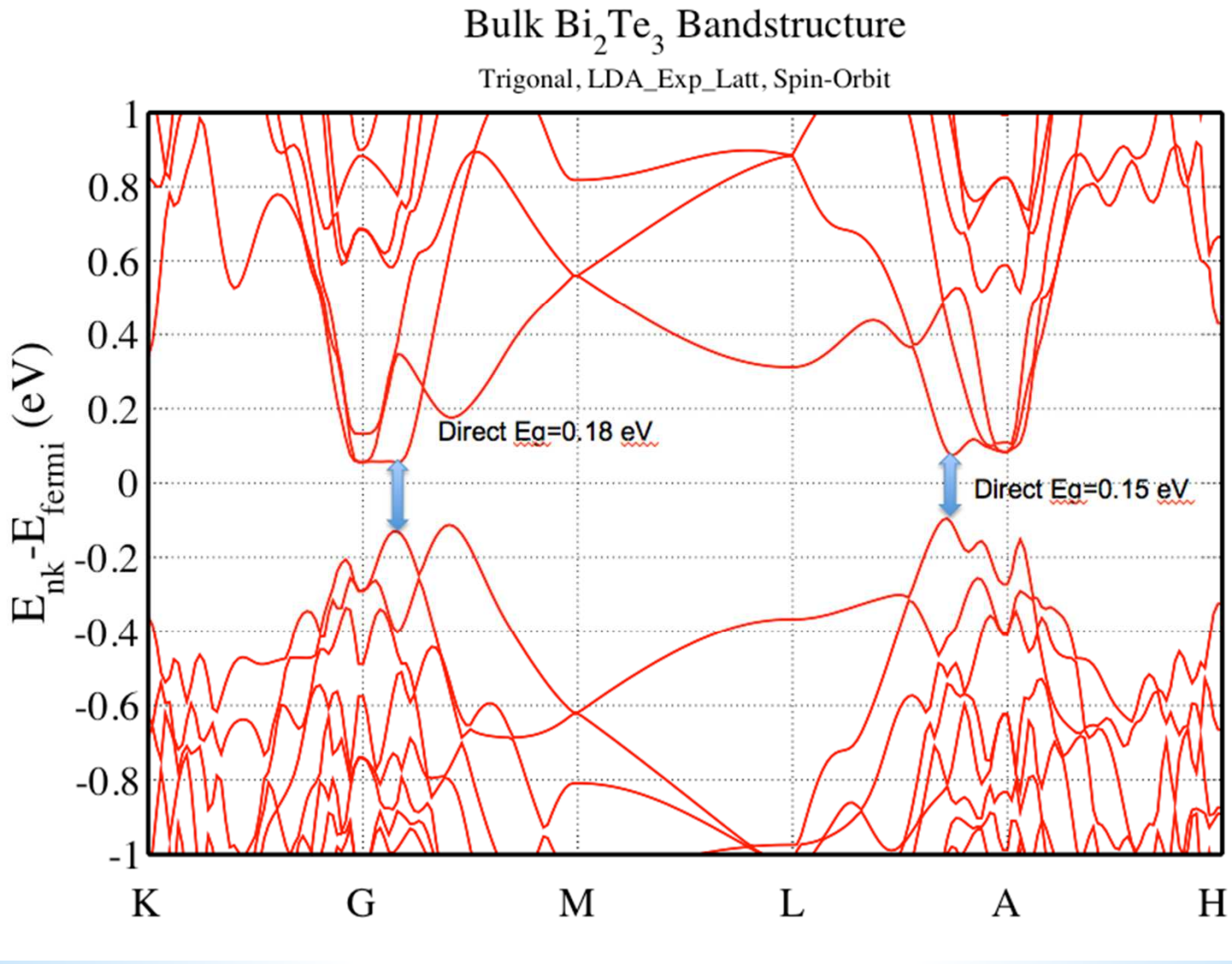
Bulk Bi_2Te_3 Bandstructure
Trigonal, LDA_Exp_Latt, Spin-Orbit
E_{nk}-E_{fermi} (eV)
1
0.8
0.6
0.4
0.2
0
-0.2
-0.4
-0.6
-0.8
-1
Direct Eg=0.18 eV
Direct Eg=0.15 eV
K
G
M
L
A
H

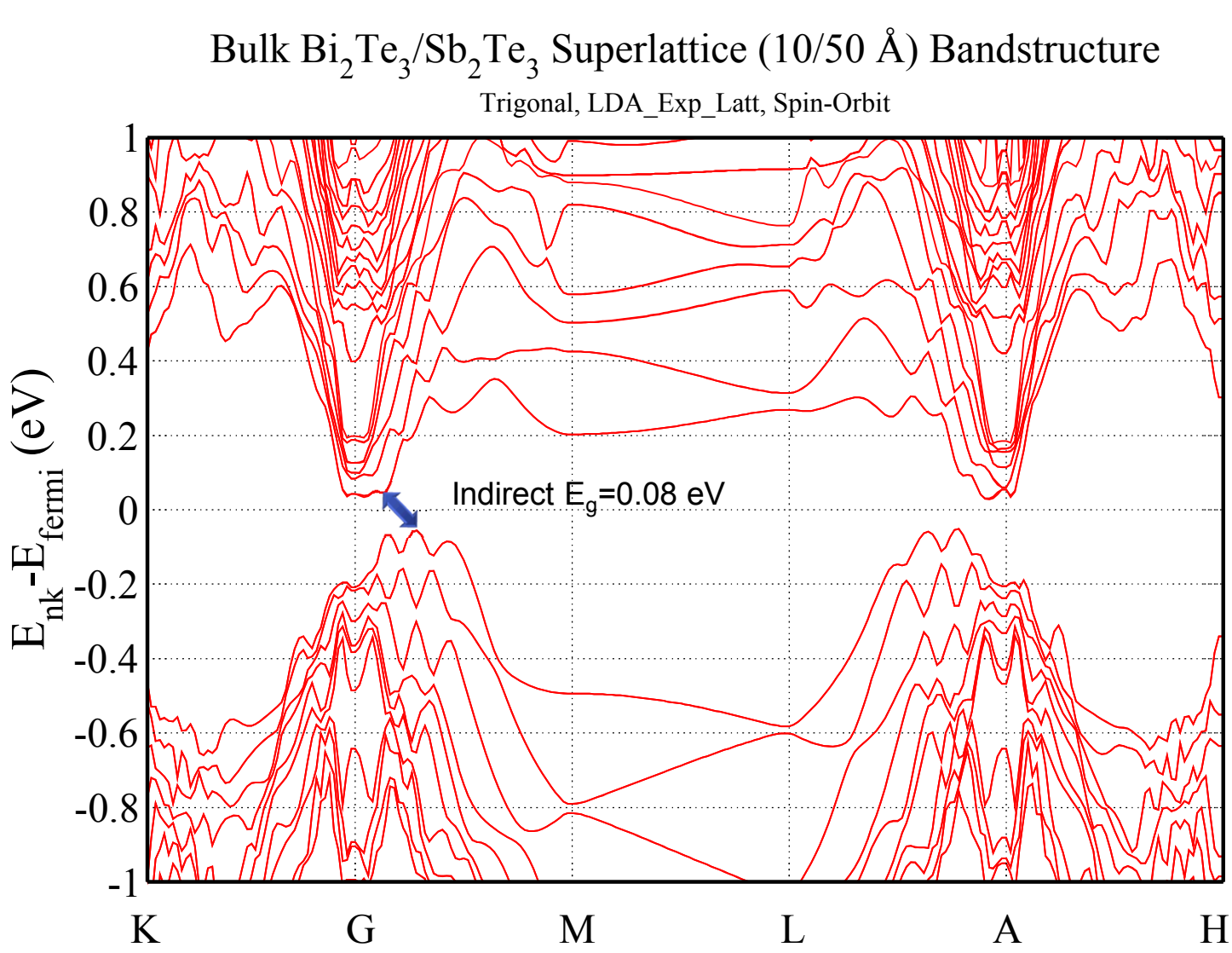
Bulk Bi_2Te_3/Sb_2Te_3 Superlattice (10/50 Å) Bandstructure
Trigonal, LDA_Exp_Latt, Spin-Orbit
E_{nk}-E_{fermi} (eV)
1
0.8
0.6
0.4
0.2
0
-0.2
-0.4
-0.6
-0.8
-1
Indirect E_g=0.08 eV
K
G
M
L
A
H

DARPA

100	110	111
Cr		
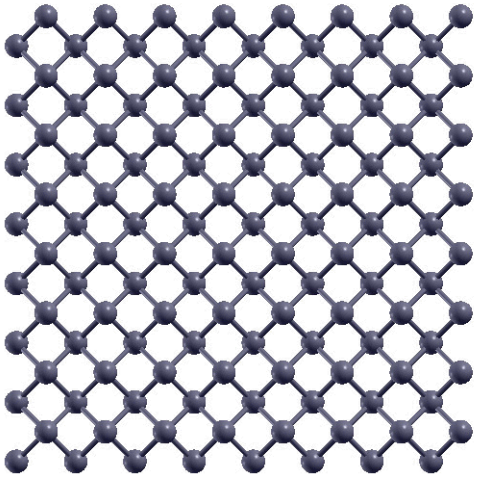	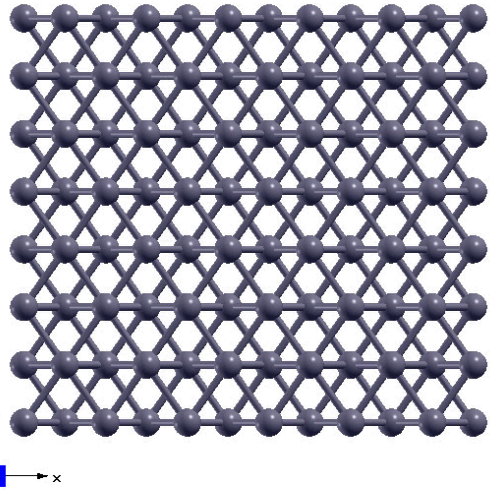	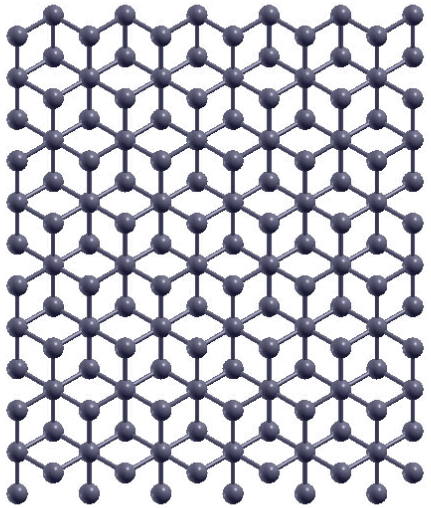
Surface atomic density 0.2378 / Å^2	Surface atomic density 0.2522 / Å^2	Surface atomic density 0.1373 / Å^2
Cr		
Bi_2Te_3		
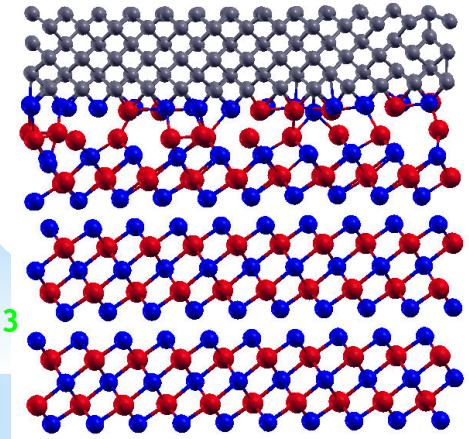	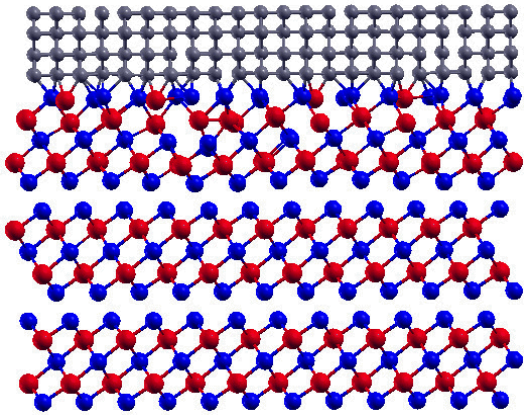	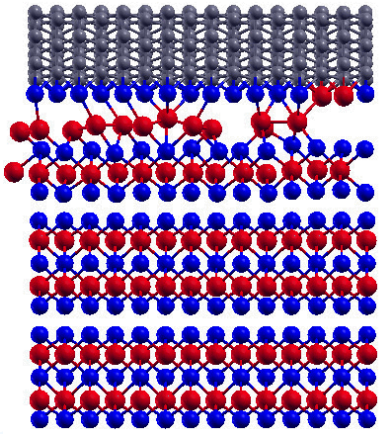

- Strong **Cr-Te interaction** + large **lattice mismatch** → interface **disorder**

- ✓ Several other semiconductor/metal interfaces have been considered:

$Sb_2Te_3/Cr(110)$

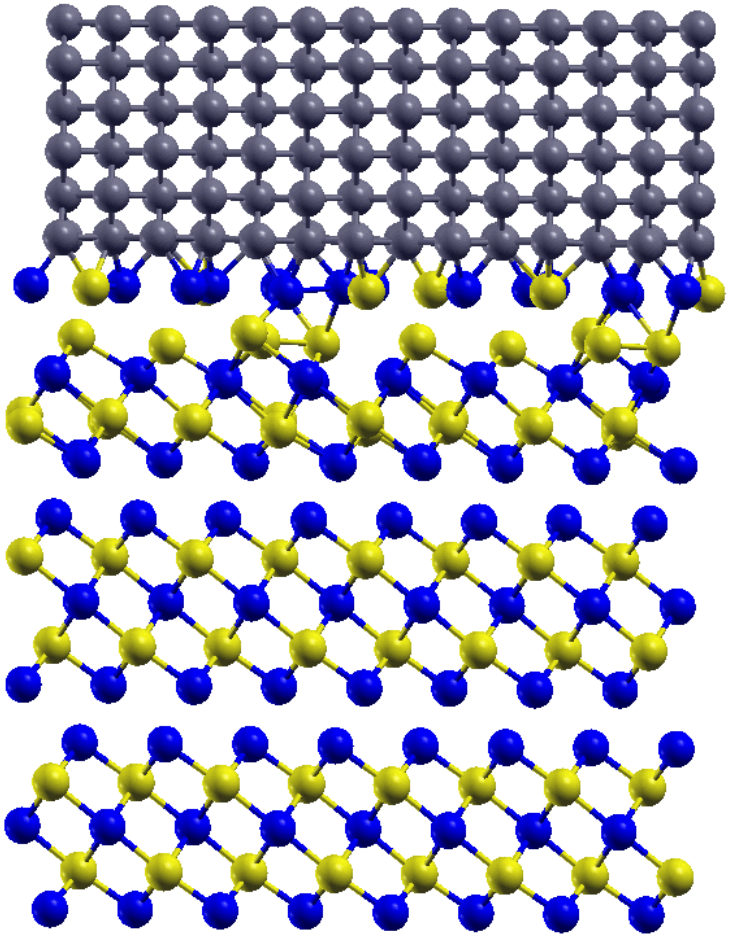

'vertical' $Bi_2Te_3/Cr(110)$

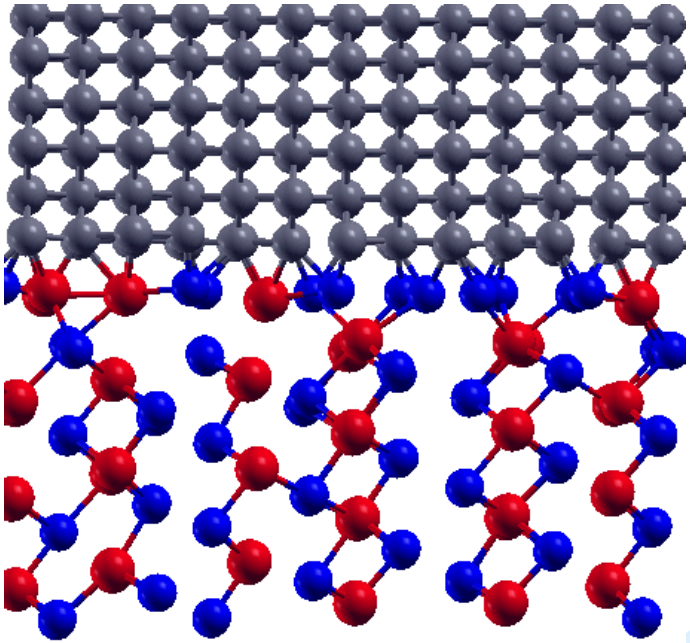

'Vertical' geometry may be relevant for interface at **step edges.**

- ✓ Several other semiconductor/metal interfaces have been considered:

Bi_2Te_3/Ti(1010)

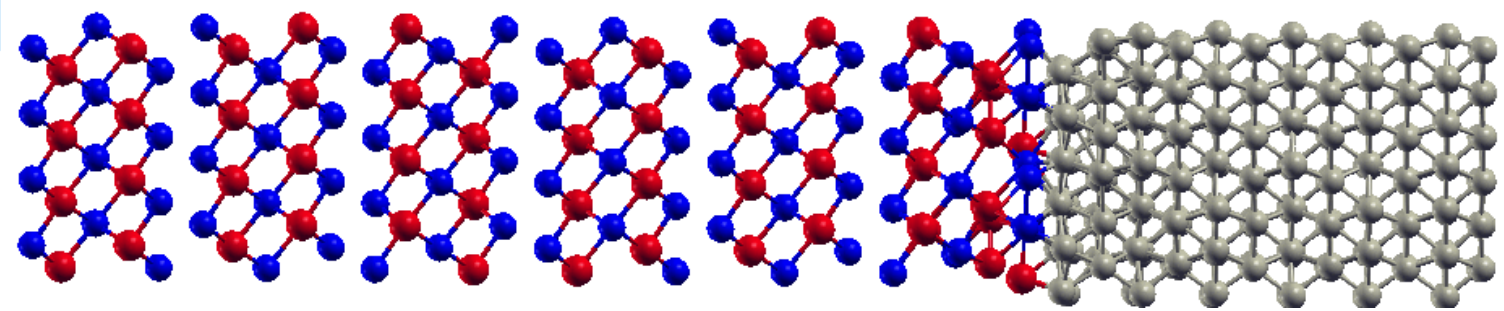

- **Ti** induces slightly **less disorder** in Bi_2Te_3 than Cr.
- - better match between hexagonal planes.

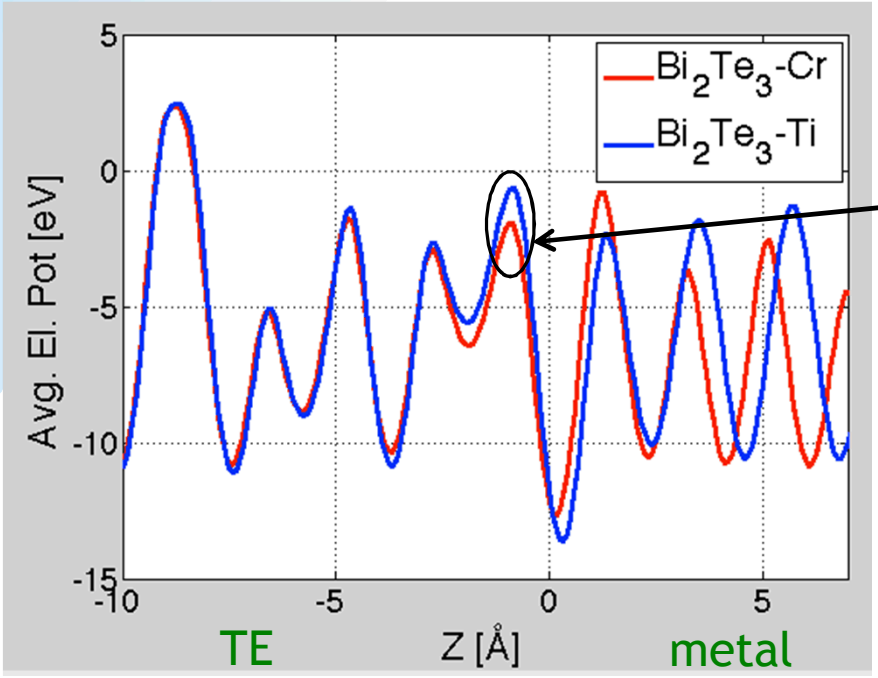

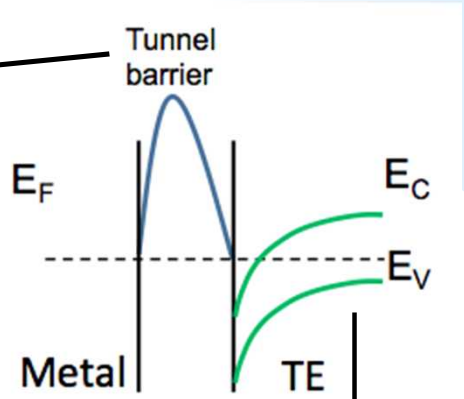

- Atomistic calculations reveal **no tuneling barrier**.
  - short bond-length between metal and TE.

How about **band bending** ?

Work Function of Metal Cr and Ti

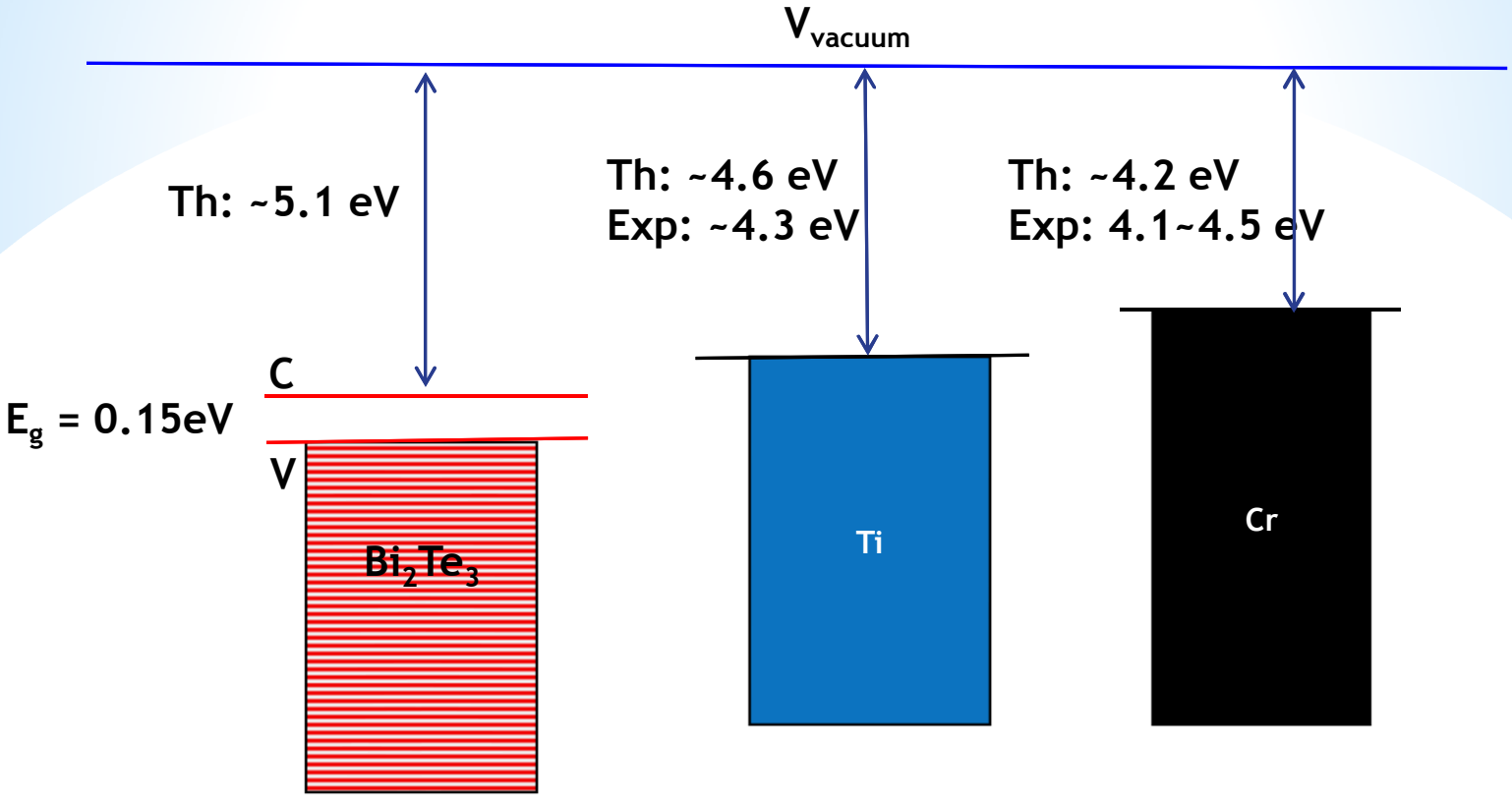

- TE-metal **chemical potential difference** drives charge transfer → band bending.
  - *chemical interaction* between Te and metal atoms also important.

All analyzed cases show similar band bending:

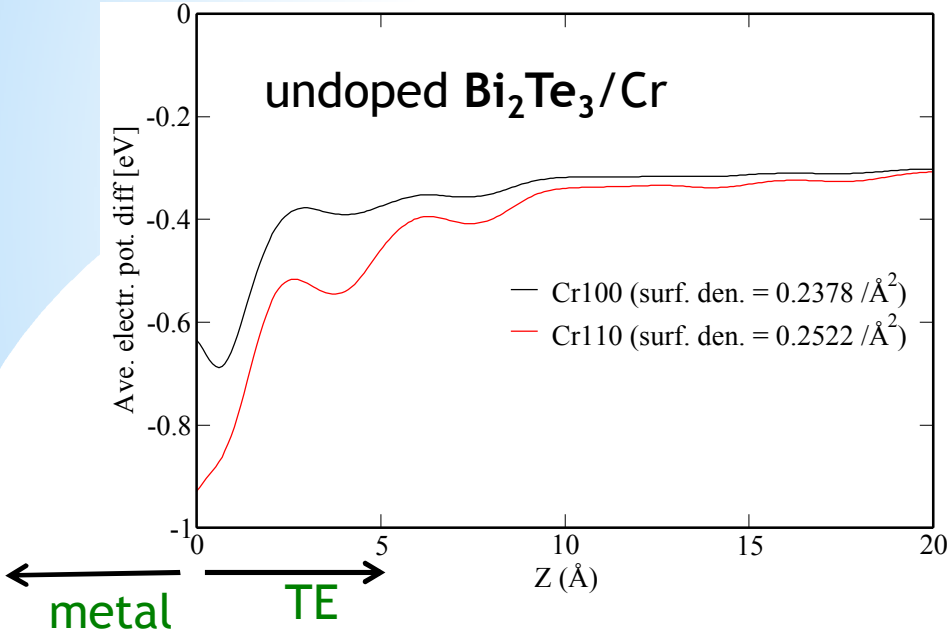

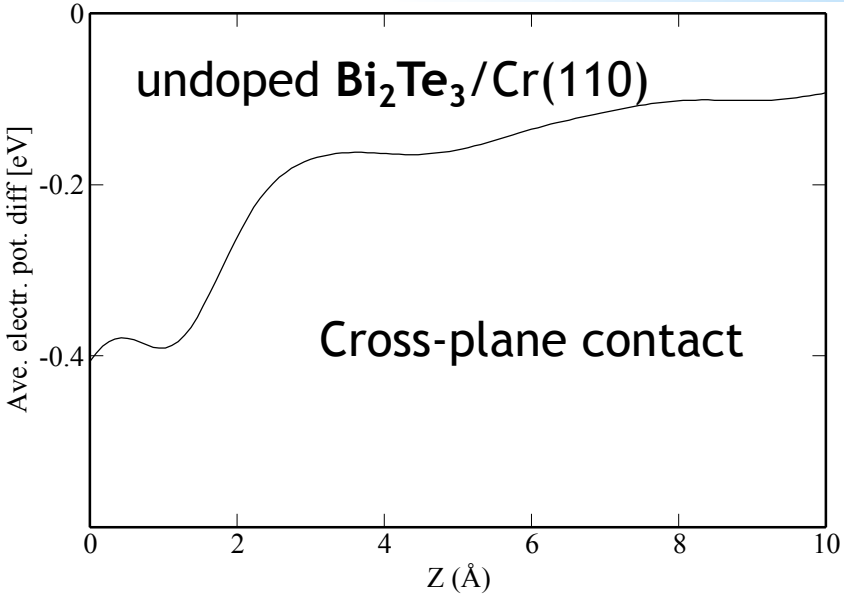

- Strong charge-transfer doping. Expect:
  - **Schottky** contact to p-type TE.
  - **Ohmic** contact to n-type TE.

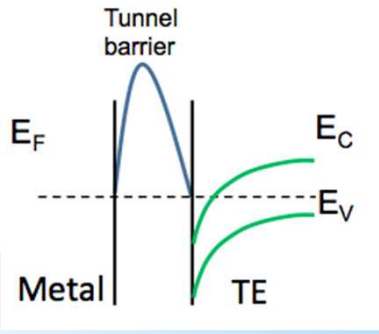

- More **disorder → smaller band bending**.
- Smaller band bending for **cross-plane** Bi_2Te_3/Cr contact.

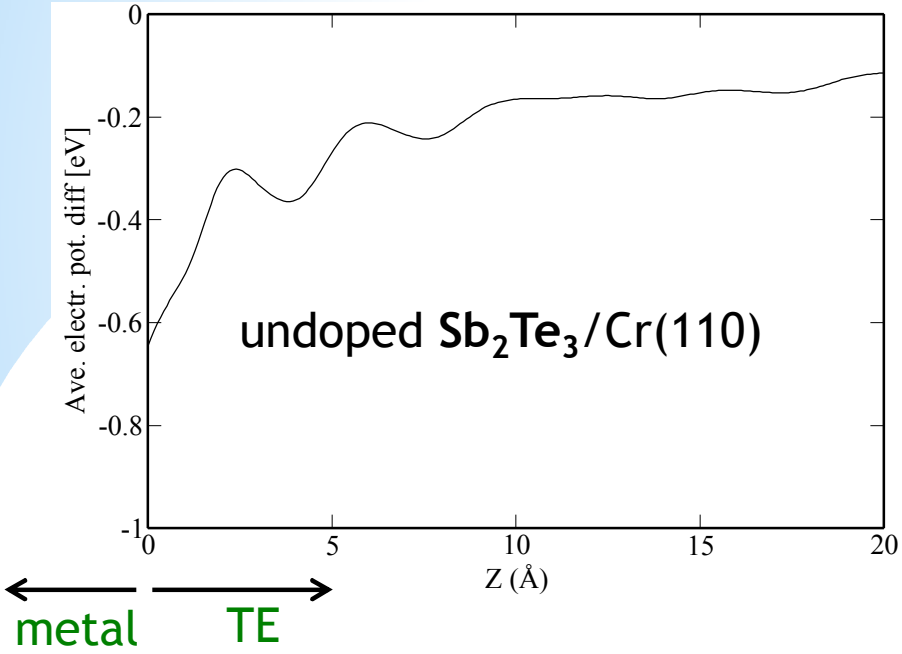

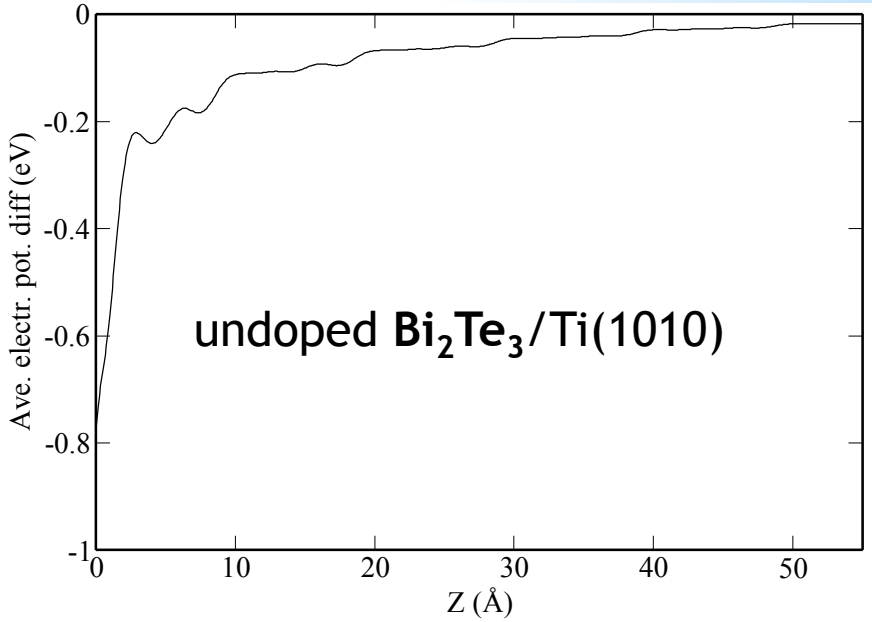

- Slightly smaller Schottky barrier for Sb_2Te_3/Cr than for Bi_2Te_3/Cr.

- **Ti**: slightly larger Schottky barrier than in **Cr** case.

DARPA

*

- ✓ Performed *ab initio* calculations of **p-doped** (anti-site defect) Sb_2Te_3 in contact with Cr.

p-doped Sb_2Te_3/Cr(110) 6.5×10^{19} holes/cm^3

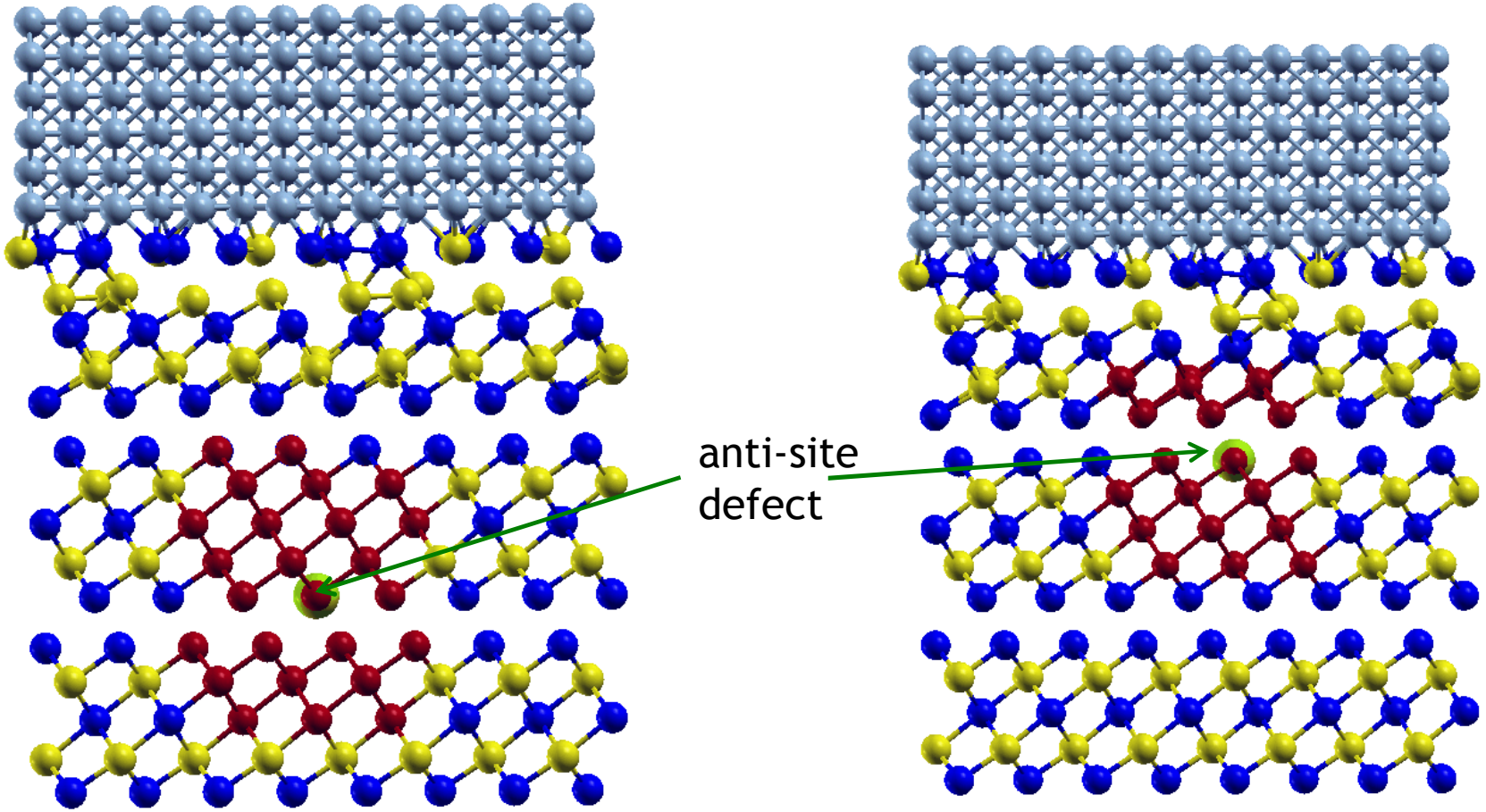

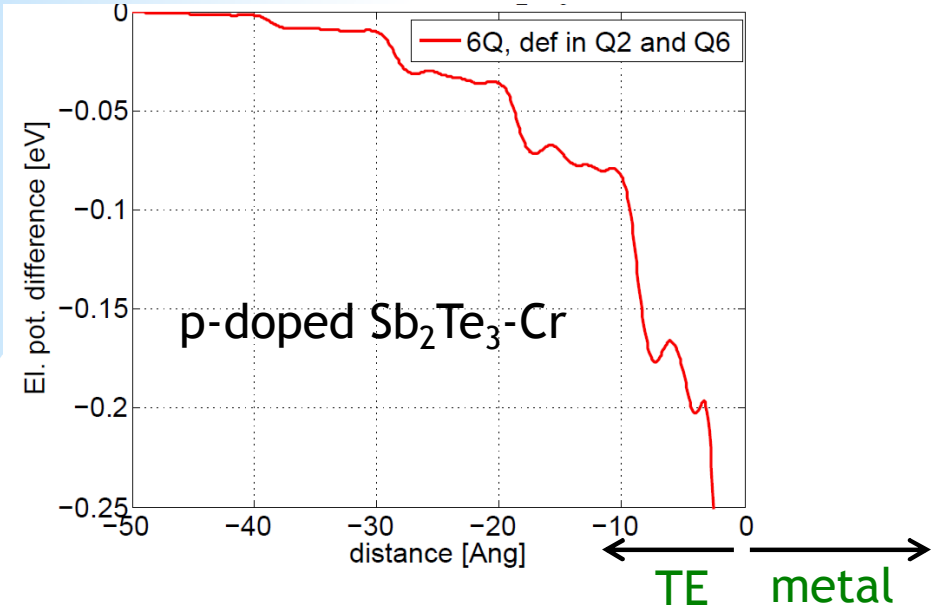

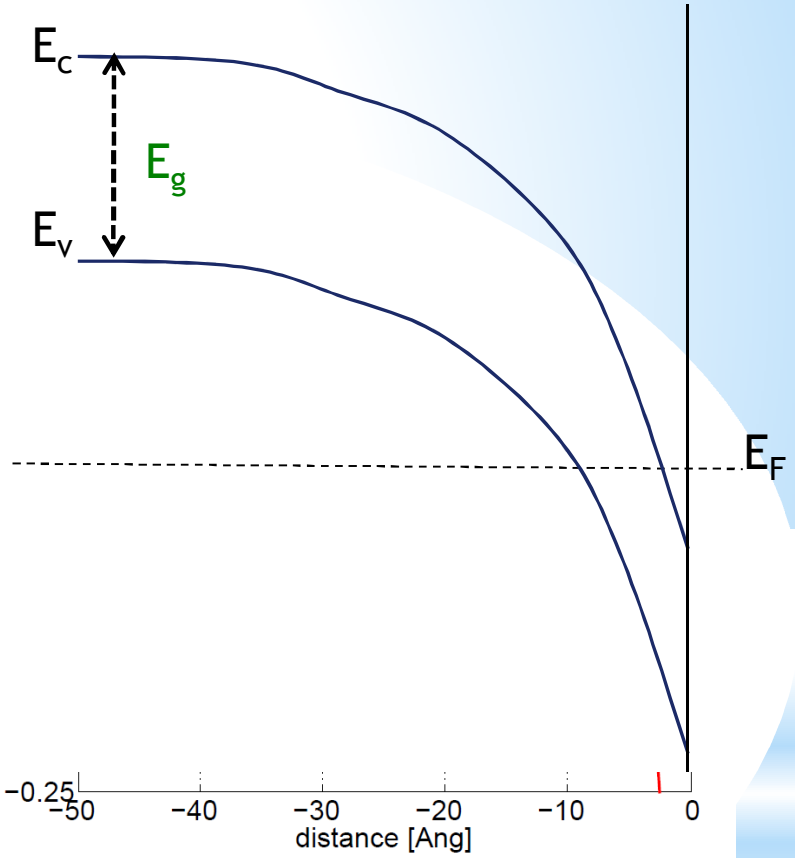

✓ Band bending potential is **not sensitive** to position of defect.

Ab initio calcs., bulk Sb_2Te_3 → **E_g=0.11 eV**

Projected spectral function:

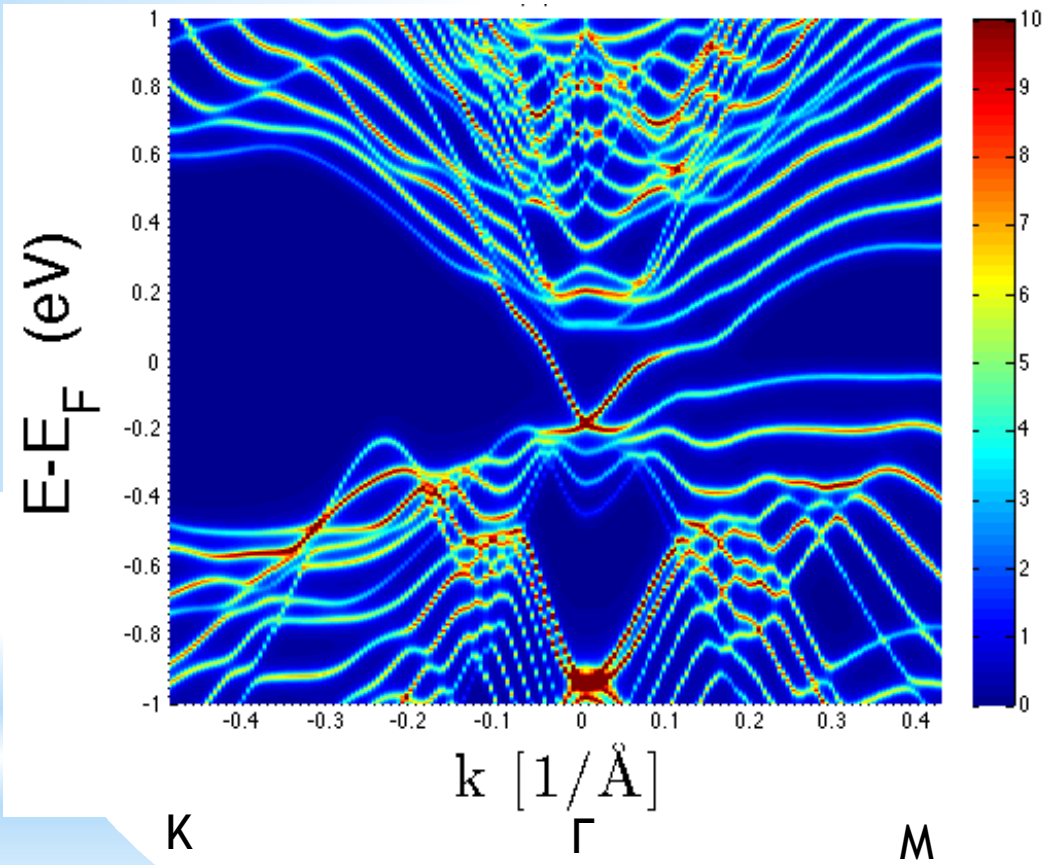

Undoped Sb_2Te_3
- quintuplet next to vacuum

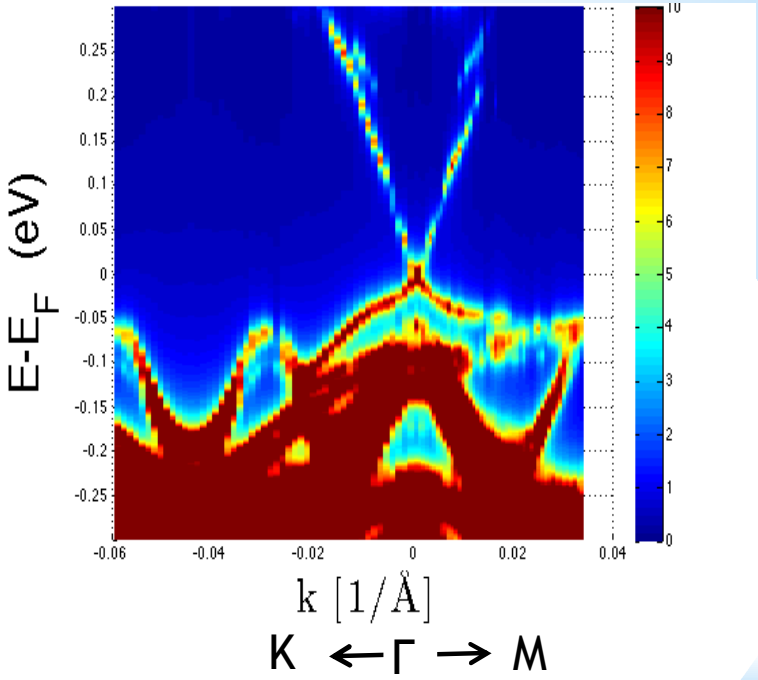

Doped Sb_2Te_3-Cr
- quintuplet next to vacuum

Compare **Dirac** point → **E_v-E_F~0.1 eV** (6.5x10^{19} holes/cm^3)

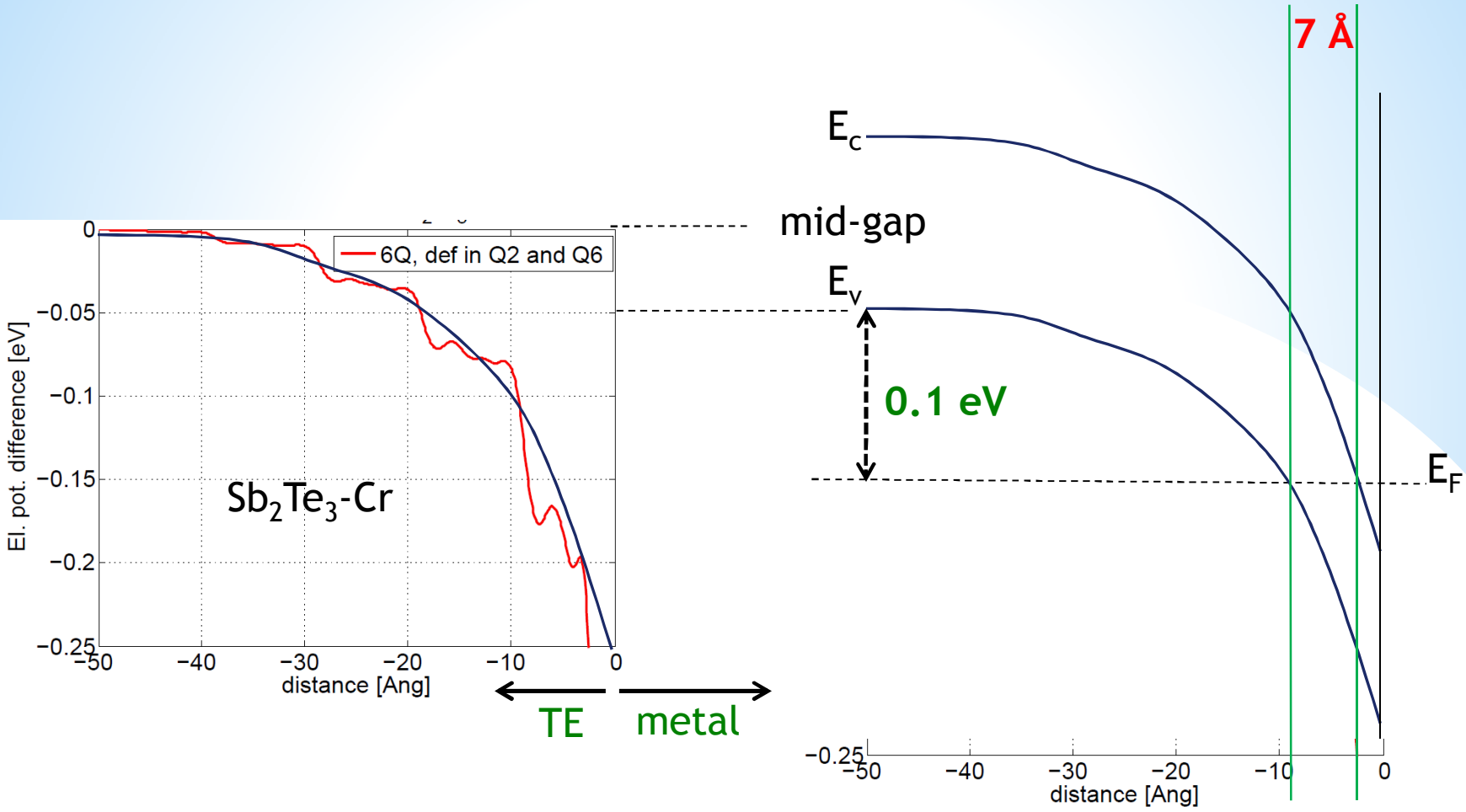

- Band-bending was obtained by drawing a smooth line manually through the red line.

* Macroscopic modeling

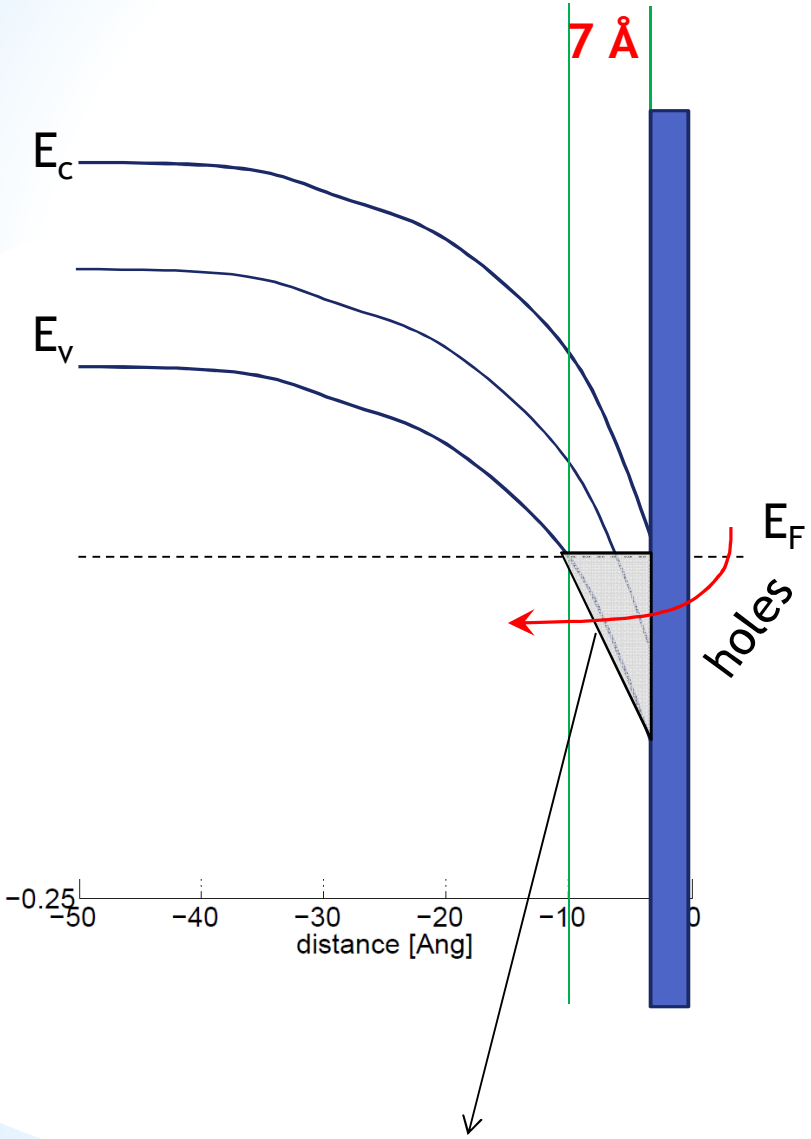

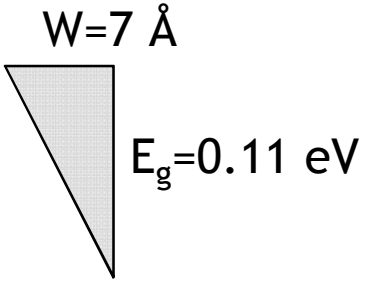

tunneling barrier

- **Developed** modeling tool based on *rigid-band model* for calculating contact resistivity.
- **Estimated** the contribution of **several mechanisms** to the contact resistance **of p-doped Sb_2Te_3/Cr** interfaces.

Thermionic contribution

$$J = A^* T^2 \exp\left(-\frac{e\phi_B}{k_B T}\right)\exp\left(\frac{eV}{k_B T}\right)$$

with the Richardson constant

$$A^* = \frac{4\pi e m^* k_B^2}{h^3}.$$

This gives the contact resistivity

$$\rho_c = \left(\frac{\partial J}{\partial V}\right)^{-1}\Bigg|_{V=0} = \frac{1}{A^* T^2}\frac{k_B T}{e}\exp\left(\frac{e\phi_B}{k_B T}\right)$$

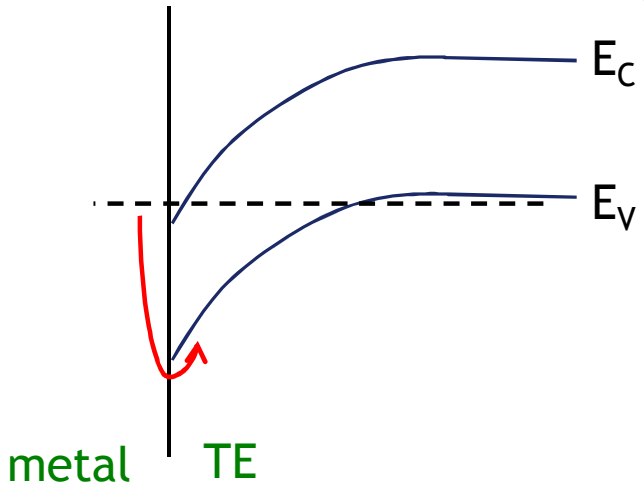

Tunneling contribution

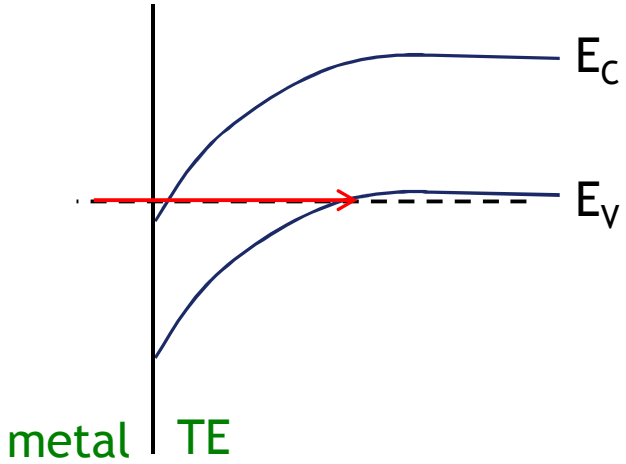

$$J = \frac{4\pi m^* e}{h^3} \int dE \left[f_M(E) - f_S(E) \right] \int P(E_x) dE_x$$

$$P(E_x) = \exp\left[-\frac{2\sqrt{2m^*}}{\hbar} \int \sqrt{eV(x) - E_x}\, dx \right]$$

Full numerical calculation of transport:

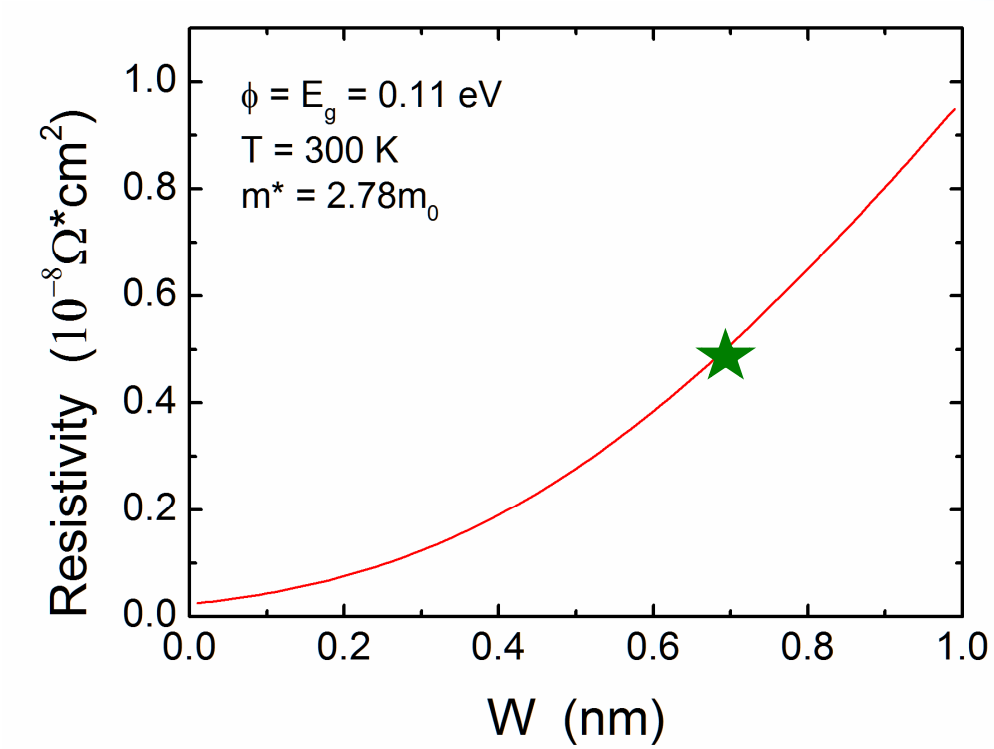

- **Thermionic field emission** is the main contribution to the current.

✓ Estimated contact resistivity at T=300 K, doping=6.5x10^{19} holes/cm^3 :

$$\rho_C \sim 5 \times 10^{-9}\,\Omega\mathrm{cm}^2$$

Lower limit for resistivity

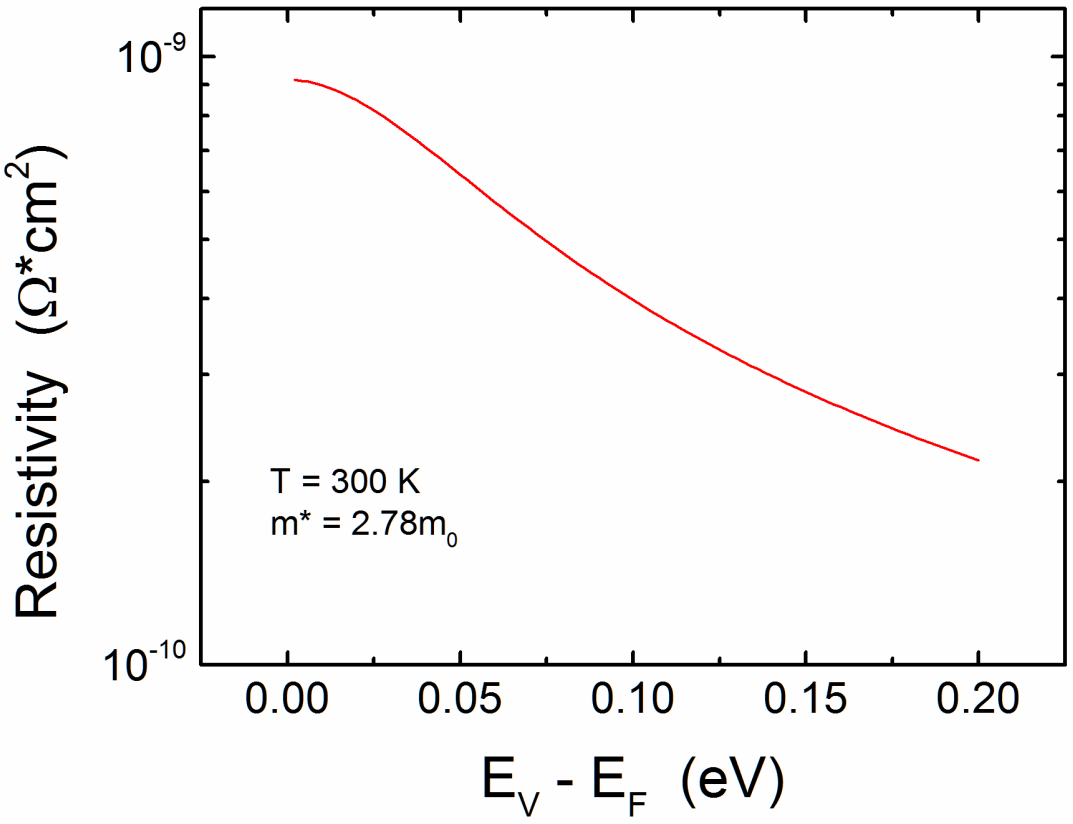

$$\rho_C^{\min} = R_0 / DOM$$

$$DOM(E) =^{1)} \frac{m^*_{DOM} E}{2\pi\hbar^2}$$

- Defined as the limit when the tunneling length and barrier height go to zero (relevant to **n-type** contacts).

1) Jeong, Kim, Luisier, Datta and Lundstrom, JAP **107**, 023707 (2010).

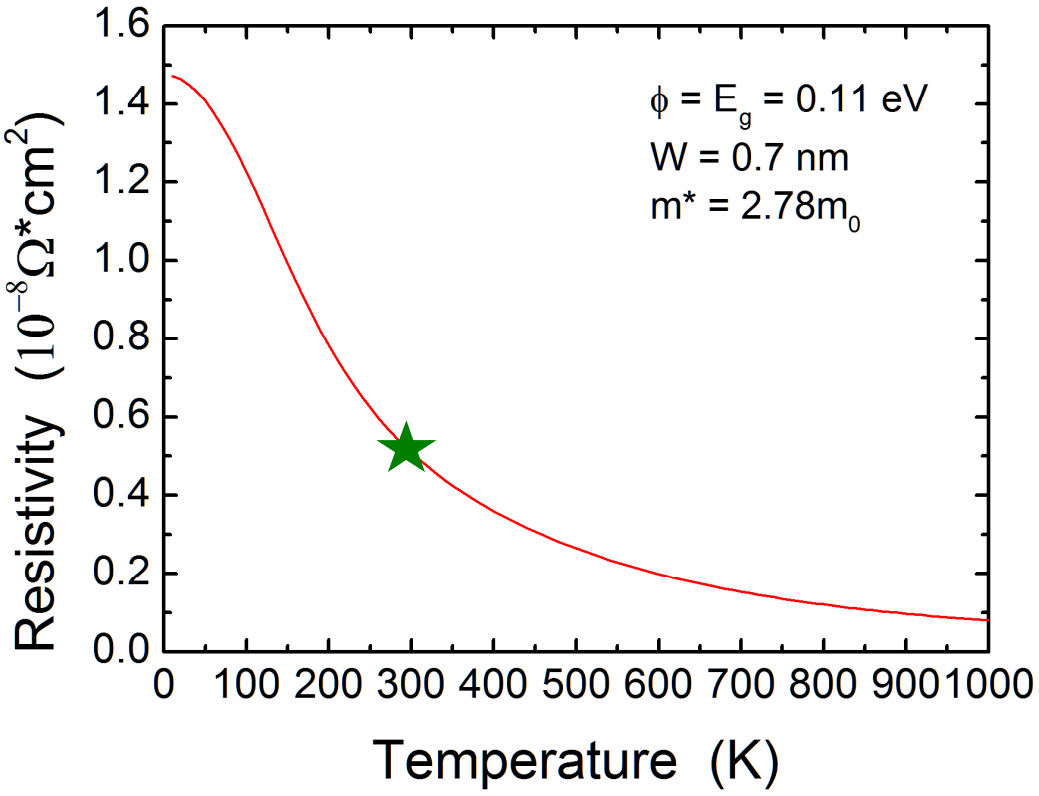
1.6
1.4
1.2
1.0
0.8
0.6
0.4
0.2
0.0
Resistivity (10^-8 Ω*cm^2)
0 100 200 300 400 500 600 700 800 900 1000
Temperature (K)
ϕ = E_g = 0.11 eV
W = 0.7 nm
m* = 2.78m_0

* Impact of disorder

* A rough estimate of contact resistivity can be obtained from the density of modes (DOM) of a **superlattice**:

$$\rho_c = R_0 / DOM(E_F)$$

- R_0=12.9 kΩ (unit of quantum resistance)

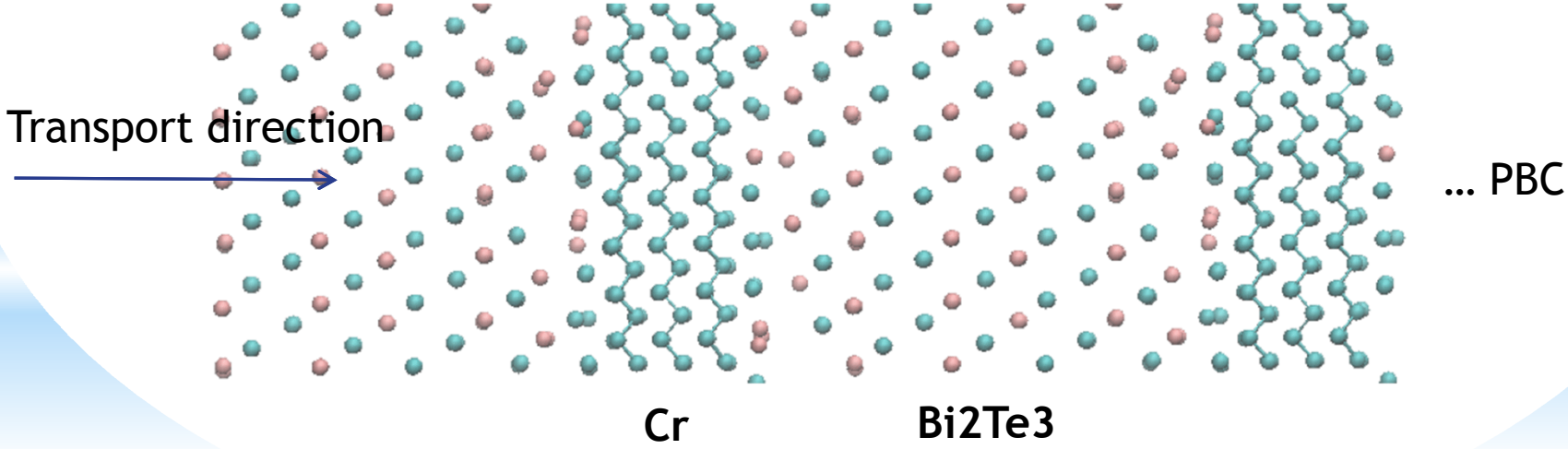

Ab initio DOM for superlattice geometry:

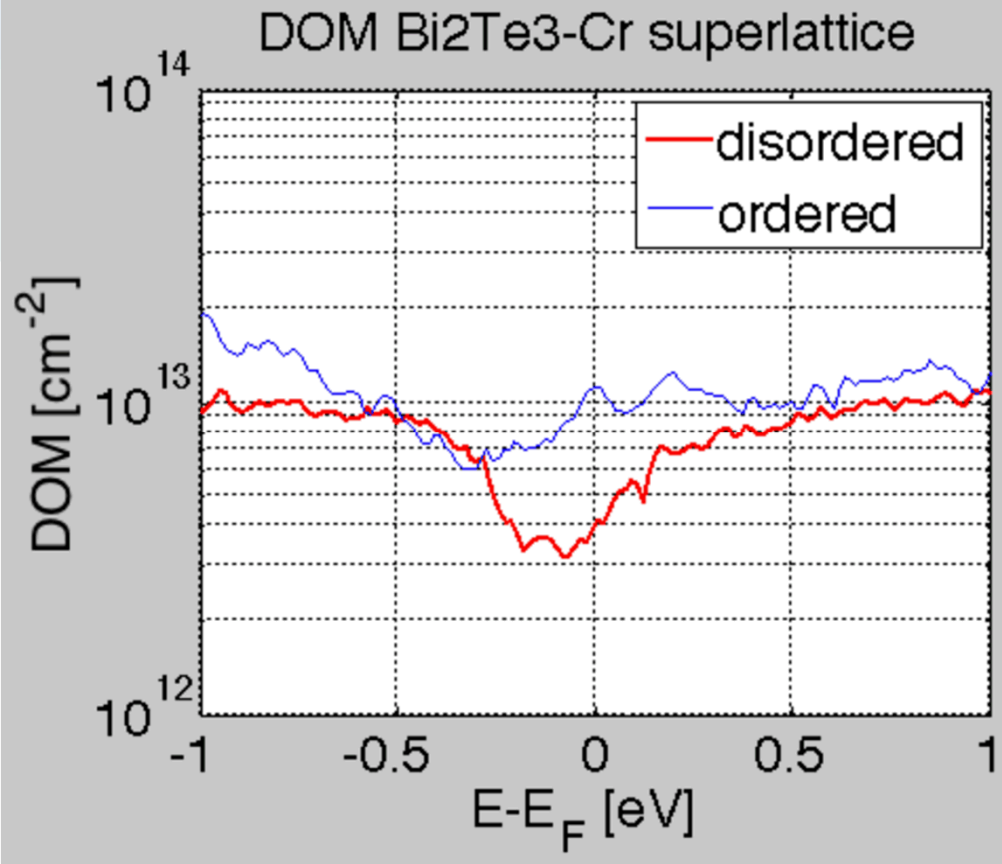

- DOM(E_F)~5x$10^{12}$$cm^{-2}$ → ρ_c=2.5x10^{-9} Ω cm^2
  - ordered interface → ρ_c gets reduced by ~40% at most.

✓ SL estimate consistent with macroscopic modeling.

Measured contact resistivity

Bulman, Barletta et al. Nature Comm. **7**, 10302 (2016):

Table 2 | Specific electric contact resistivity, as measured by transmission line model (TLM) technique, for superlattice thermoelectric elements with different structures and metallization.

Sample	Growth information		Contact metal	Contact resistivity		
	Type	Target structure		R_s (Ω per sq)	L_T (μm)	ρ_C (Ω cm^2)
A	n	δ-doped n type	Plated Au	1.57	4.20	2.68e-7
B	p	Bi_2Te_3/Sb_2Te_3	Plated Au	0.93	12.26	1.36e-6
C	n	δ-doped n type	Evap Cr/Ni/Au	1.94	7.81	1.16e-6
D	p	Bi_2Te_3/Sb_2Te_3	Evap Cr/Ni/Au	1.15	11.74	1.42e-6

Evap, evaporated.

- Measured ρ_c ~ 10^{-7} to $10^{-6}\Omega cm^2$ → higher than theory estimate (for similar doping levels ~ 10^{19} holes/cm^3).

  ✓ Theory suggests that **clean** $(Bi,Sb)_2Te_3$/Cr interfaces should have **lower** contact resistance:

  → Original goal of $\rho_C \leq 10^{-8}\ \Omega cm^2$ can be achieved.

* TEM analyses

EDS mapping at interface

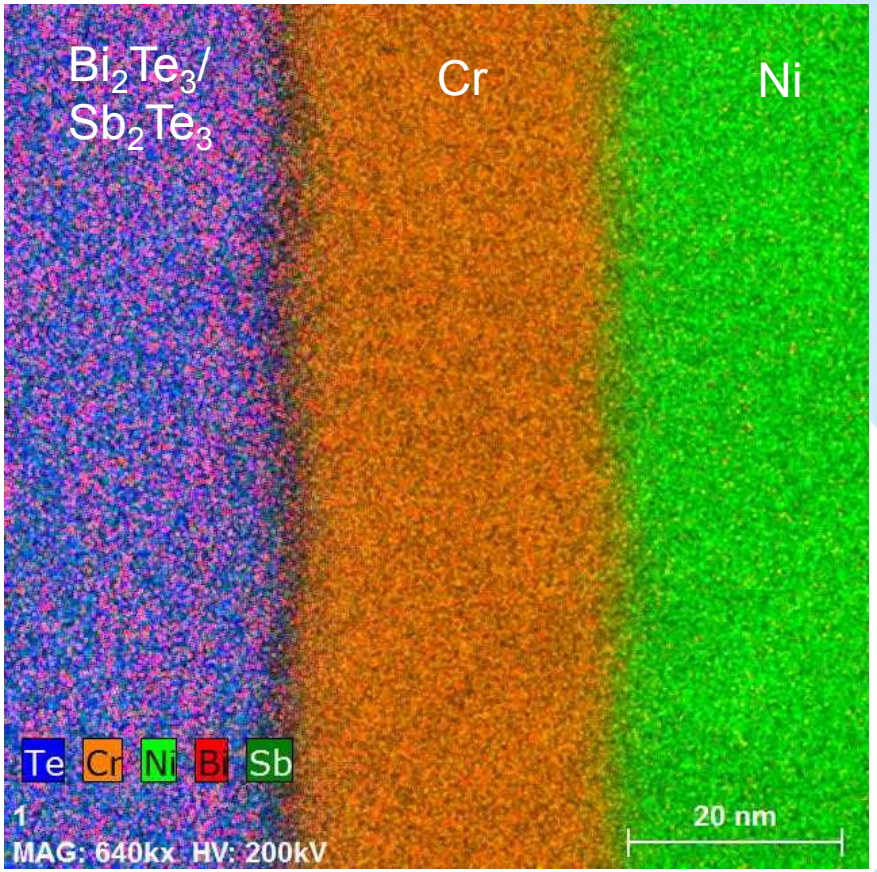

TEM analysis suggested a **thin interfacial layer** between the Cr contact and the $(Bi,Sb)_2Te_3$ material.

- In conjuction with **theory** results, we hypothesize that this might be an **oxide layer**.

* End

Good progress towards understanding the limits of **low-ρ_C** in realistics metal-contacts to TE.

Acknowledgements

Work supported by **DARPA-MATRIX** program.